Journal of Nonlinear Modeling and Analysis
Volume 7, Number 4, August 2025, 1206–1239
https://journal.global-sci.org/jnma
DOI:10.12150/jnma.2025.1206

Fibonacci Wavelet Collocation Method for Solving a Class of System of Nonlinear Pantograph Differential Equations

Manohara G[1] and Kumbinarasaiah S[1,†]

Abstract This paper introduces a unique strategy for solving numerically a class of nonlinear Pantograph differential equations using the Fibonacci wavelet collocation method (FWCM). First, we transform the nonlinear Pantograph differential equations system into a nonlinear algebraic system using this proposed approach. Next, the transformed nonlinear algebraic system is solved by using the Newton-Raphson scheme. The main advantage of this approach lies in its ability to reduce the computational complexity associated with solving Pantograph equations, resulting in accurate and efficient solutions. Comparative analyses with other established numerical methods reveal its superior accuracy and convergence rate performance. Further, a few examples are provided to evaluate the effectiveness of the suggested approach using absolute error functions. As far as our literature survey indicates, no one attempted the nonlinear Pantograph differential equations by FWCM. It compels us to study a system of Pantograph differential equations via FWCM.

Keywords Pantograph equations, collocation technique, Fibonacci wavelet, operational matrix of integration

MSC(2010) 34A08, 34A34, 34K28, 78A70, 93A30.

1. Introduction

Differential equations have been vital for defining and analyzing problems in many scientific disciplines for more than 300 years. The concepts of differential equations were initially introduced in the late seventeenth century by Gottfried Wilhelm Leibniz, Isaac Newton, and the Bernoulli brothers, Johann and Jakob. These happened naturally from these outstanding scientists' attempts to apply the new concepts of calculus to specific mechanical issues, such as the brachistochrone problem and celestial body motion routes. From the earliest ways of finding exact solutions in terms of elementary functions to the more recent methods of analytic and numerical approximation, their significance has inspired generations of mathematicians and other scientists to develop methods for investigating features of their solutions. Furthermore, they have been essential to the growth of mathematics since discoveries in analysis, topology, algebra, and geometry have frequently provided fresh insights into differential equations and since queries concerning differential equations have given rise to new fields of study.

[†]the corresponding author.
Email address: kumbinarasaiah@gmail.com
[1]Department of Mathematics, Bangalore University, Bengaluru-560 056, India

Systems of ordinary differential equations are often encountered in different science fields, such as biology, physics, economics, and engineering. Due to their versatility in modeling and describing dynamic processes, systems of ordinary differential equations (SODEs) find extensive use in diverse domains. Ordinary differential systems are essential tools to solve problems in the real world. ODE system of second order describes a broad range of natural phenomena. For instance, chemists can forecast reaction rates as well as the concentrations of reactants and products over time by using ODEs to simulate the kinetics of chemical processes, to comprehend and predict the behavior of economic variables like inflation, GDP growth, and investment. ODE systems are employed in financial modeling, and climate models use ordinary differential equations (ODEs) to forecast the earth's temperature, precipitation patterns, and other climatic variables throughout time.

The differential equations that describe the motion of a pantograph are crucial for understanding and analyzing the behavior of the mechanical linkage. These equations are significant for the following reasons: The differential equations make it easier to comprehend how the pantograph's orientation and position vary over time in response to outside inputs and forces. Forecasting and examining the pantograph's motion while it is in operation is necessary. Pantographs are sometimes employed with control systems to accomplish particular motion patterns or to follow a predetermined path. The differential equations play a crucial role in developing and applying control algorithms that regulate the pantograph's movement. The basics for developing mathematical models of pantograph systems are differential equations. Engineers can test theories, investigate alternative scenarios, and assess the pantograph's performance under various circumstances by using these models for simulation. Pantograph differential equations are significant because they are a vital tool for evaluating, planning, and enhancing the motion of pantograph systems in various applications.

Consider the following class of system of nonlinear Pantograph differential equations. [1]

$$\begin{aligned}
\mathscr{Z}_1'(\xi) &= \alpha_1 \mathscr{Z}_1(\xi) + f_1(\xi, \mathscr{Z}_i(\xi), \mathscr{Z}_i(q_j\xi)),\\
\mathscr{Z}_2'(\xi) &= \alpha_2 \mathscr{Z}_2(\xi) + f_2(\xi, \mathscr{Z}_i(\xi), \mathscr{Z}_i(q_j\xi)),\\
&\vdots\\
\mathscr{Z}_n'(\xi) &= \alpha_n \mathscr{Z}_n(\xi) + f_n(\xi, \mathscr{Z}_i(\xi), \mathscr{Z}_i(q_j\xi)).
\end{aligned} \tag{1.1}$$

$u_i(0) = u_{i_0}$, where $i, j = 1, \ldots, n$, $\alpha_i, u_{i_0} \in \mathbb{R}$, f_i are analytic functions, and $0 < q_j < 1$. $\mathscr{Z}_i(\xi)$ are dependent variables and ξ is an independent variable.

Multiple numerical approaches are created to approximate the solutions to those equations because of the challenges in finding the analytical solutions. Widatalla S. implemented the Laplace transform and Adomian decomposition method [1], Khuri S., [2] proposed the Laplace Adomian decomposition method, Cakmak M. et al. implemented the Fibonacci collocation method [3], He et al. proposed variational iteration method [4], Operational matrix approach based on Bernoulli polynomials was proposed by Rani D. et. al. [5], Odibat et al. developed Optimized decomposition method [6] and improved optimal homotopy analysis algorithm [7]. Davaeifar S., proposed the first Boubaker polynomials (FBPs) for the multi pantograph type equations [8].

2. Wavelet theory

A relatively new area of mathematics is wavelet theory and wavelet analysis. Alfred Haar created the first and most basic wavelet in 1909. It was initially used in the 1980s for signal processing, and in the last ten years, its enormous potential for image processing applications has been acknowledged. Fourier transforms can be used to extract frequency information. Eventually, however, it loses its association with any spatial data. Wavelet transforms can extract precise information from one image, which can be injected into another using various techniques, such as addition, substitution, or selection based on spatial context or frequency. Additionally, the wavelet function employed in the transform might be created with special qualities beneficial for the particular transform application. In particular, the literature frequently employs orthogonal wavelets to handle various differential equations. Several wavelet-based numerical approaches have been magnificently solved in the literature, including the following: Legendre wavelet collocation method [9, 10], Taylor wavelet collocation method [11, 12], Hermite wavelet collocation scheme [13, 14], Chebyshev wavelet collocation method [15, 16], Laguerre wavelet collocation approach [17, 18], Bernoulli wavelet scheme [19, 20, 22], Ultraspherical wavelet method [23, 24], Cardinal B-spline wavelet method [25], Genocchi wavelets [26] and Gegenbauer wavelet method [27].

Fibonacci wavelets are derived from Fibonacci polynomials, one of the essential members of Appell polynomials. The Fibonacci wavelet basis functions possess remarkable properties, including compact support, making them well-suited for approximating solutions to differential equations. Fibonacci polynomials are advantageous when approximating functions over classical orthogonal polynomials such as Chebyshev and Laguerre polynomials because of fewer terms and smaller coefficients of individual terms. An extensive discussion is included in the book [28] regarding the properties, benefits, applications, and various other extensions of Fibonacci polynomials. The suggested wavelet-based numerical method is easy to implement, computationally attractive, efficient, and computationally appealing. Because of its unique characteristics and benefits over other wavelets, Fibonacci wavelets have drawn the interest of many researchers. As a consequence, the researchers used this polynomial-based wavelet method to solve some of the equations, such as telegraph equations in a fractional sense with Dirichlet boundary conditions [29], epidemiological model of computer virus [30], fractional optimum control problems with bibliometric analysis [31], time fractional bioheat transfer model [32], chemistry problems [33], two types of time-varying delay problems [34], a category of nonlinear differential equation systems [35], Penne's bioheat transfer equation [36], fractional order Brusselator chemical model [37], higher order linear Fredholm integral differential-difference equations [38], fractional partial differential equations arising in the financial market [39], distributed-order fractional optimal control problems [40]. Some of the articles utilized to improvise the paper are [45–51].

2.1. Significance of the proposed method (FWCM)

1. Fibonacci wavelets are a special type of wavelets that are not based on orthogonal polynomials. Still, we can express the Fibonacci polynomials in terms of some orthogonal polynomials, such as the Chebyshev polynomial of the

second kind.

2. The Fibonacci polynomials have fewer terms than Legendre polynomials. This difference increases with an increase in the degree of polynomial. Therefore, Fibonacci polynomials take less CPU time than Legendre polynomials.
3. Error components in the OMI representing Fibonacci polynomials are less than those of other polynomials, i.e., the Fibonacci polynomials have smaller coefficients of individual terms than corresponding ones in other polynomials. Computational errors can be reduced using this property.
4. The coefficients of the Fibonacci polynomial are found very easily by using computer programs like the $Fibonacci[m, x]$ command implemented in Mathematica to obtain Fibonacci polynomials.
5. The Fibonacci wavelet method is suitable for solutions with sharp edge/ jump discontinuities.
6. Fractional differential equations, delay differential equations, and stiff systems can be solved using this method directly without using any control parameters.
7. By slightly modifying the method, the Fibonacci wavelet method can be used to solve the higher-order system of ordinary differential equations.
8. This method can also be extended to PDEs and other mathematical models with different physical conditions.
9. It obtains the solution of the differential equation in the universal domain by taking the suitable transformation.

Section 3 describes the properties of Fibonacci wavelets, setting the stage for the remainder of the article. In section 4, the operational matrix for Fibonacci wavelets is shown. The solution method is presented in 5. In 6, numerical outcomes are displayed. Section 7 concludes with some findings.

3. Preliminaries of Fibonacci wavelets

On the interval $[0, 1]$, Fibonacci wavelets are defined as [29, 34],

$$\delta_{n,m}(\xi) = \begin{cases} \frac{2^{\frac{k-1}{2}}}{\sqrt{S_m}} P_m(2^{k-1}\xi - \widehat{n}), \frac{\widehat{n}}{2^{k-1}} \leq \xi < \frac{\widehat{n}+1}{2^{k-1}}, \\ 0, \qquad \text{Otherwise}, \end{cases}$$

with

$$S_m = \int_0^1 (P_m(\xi))^2 d\xi,$$

where $P_m(\xi)$ is the Fibonacci polynomial of degree $m = 0, 1, ..., M-1$, translation parameter $n = 1, 2, ..., 2^{k-1}$ and k represents the level of resolution $k = 1, 2, ...$, respectively. The quantity $\frac{1}{\sqrt{S_m}}$ is a normalization factor. The Fibonacci polynomials are defined as follows in the form of the recurrence relation for every $\xi \in R^+$,

$$P_{m+2}(\xi) = \xi P_{m+1}(\xi) + P_m(\xi), \ \forall m \geq 0,$$

with initial conditions $P_0(\xi) = 1$, $P_1(\xi) = \xi$. Fibonacci wavelets are compactly supported wavelets formed by Fibonacci polynomials over the interval $[0, 1]$.

Theorem 3.1. *[20] Let L^2[0,1] be the Hilbert space generated by the Fibonacci wavelet basis. Let $\eta(\xi)$ be the continuous bounded function in $L^2[0,1]$. Then the Fibonacci wavelet expansion of $\eta(\xi)$ converges with it.*

Theorem 3.2. *[21] Let $S = \{\delta_{i,j}(\xi) \,|\, i,j \in \mathbb{Z}\}$ be the set of Fibonacci wavelet functions on $\mathbb{R}$. Then $L^2(\mathbb{R})$ is the Fibonacci space generated by S, and it is complete.*

Proof. Let $\{\delta_{i,j}(\xi)|i,j \in \mathbb{Z}\}$, to be the basis of the normed linear space $L^2(\mathbb{R})$. Consider $\{\delta^k_{i,j}\}$ be the Fibonacci cauchy sequence in $L^2(\mathbb{R})$. By the definition of Cauchy sequence for a given, $\epsilon = \frac{1}{2} > 0$, there exists a positive integer η_1, such that $||\delta^k_{i,j} - \delta^l_{i,j}||_2 < \frac{1}{2}$, $\forall k,l \geq \eta_1$;
for $\epsilon = \frac{1}{2}$, choose $\delta^{k_1}_{i,j}$, such that $||\delta^{k_1}_{i,j} - \delta^{k_2}_{i,j}||_2 < \frac{1}{2}$, $\forall k_1, k_2 \geq \eta_1$;
for $\epsilon = \frac{1}{2^2}$, choose $\delta^{k_2}_{i,j}$, such that $||\delta^{k_2}_{i,j} - \delta^{k_3}_{i,j}||_2 < \frac{1}{2^2}$, $\forall k_2, k_3 \geq \eta_2$;

$$\vdots$$

for $\epsilon = \frac{1}{2^n}$, choose $\delta^{k_n}_{i,j}$ such that $||\delta^{k_n}_{i,j} - \delta^{k_{n+1}}_{i,j}||_2 < \frac{1}{2^n}$, $\forall k_n, k_{n+1} \geq \eta_n$.

Therefore, $\{\delta^{k_n}_{i,j}\}$ is a subsequence of $\{\delta^k_{i,j}\}$. It is clear that, $\sum\limits_{k=1}^{\infty} ||\delta^{k_{n+1}}_{i,j} - \delta^{k_n}_{i,j}||_2 \leq \sum\limits_{n=1}^{\infty} \frac{1}{2^n} = 1$.

Consider, $\phi_n = |\delta_{k_1}| + |\delta_{k_2} - \delta_{k_1}| +, ..., +|\delta_{k_{n+1}} - \delta_{k_n}|$, for $n = 1, 2, 3, ...$ Then $\{\phi_n\}$ is an increasing sequence of non-negative measurable functions, such that $||\phi_n||_2^2$=$[||\delta_{k_1}||_2 + \sum\limits_1 ||\delta_{k_{n+1}} - \delta_{k_n}||_2]^2$, (by Minkowski inequality)
$||\phi_n||_2^2 \leq (||\delta_{k_1}||_2 + 1)^2 < \infty$.

Therefore ϕ_n is a bounded and increasing sequence, then there exists ϕ such that $\lim\limits_{n\to\infty} \phi_n = \phi$. By monotone convergence theorem, we have

$$\int \phi^2 d\xi = \lim_{n\to\infty} \int \phi_n^2 d\xi < \infty \implies \phi \in L_p(\mathbb{R}).$$

This implies that the series $\delta_{k_1}(\xi) + \sum\limits_1^{\infty} |\delta_{k_{n+1}}(\xi) - \delta_{k_n}(\xi)|$ converges almost everywhere.

Therefore $\{\delta_{k_n}\}$ converges to $\delta(\xi)$, $\forall \xi \in A$, where A is a measurable set. Further, let $\epsilon > 0$ be given. Choose l so large such that $||\delta^k_{i,j} - \delta^l_{i,j}||_2 < \epsilon$, $\forall k, l \geq L$.

This implies that $||\delta^k_{i,j} - \delta^{l_n}_{i,j}||_2 < \epsilon$, $\forall k, l_n \geq L$.

Thus, we have $[\int |\delta^k_{i,j} - \delta^{l_n}_{i,j}|^2 d\xi] < \epsilon^2$ (by Fatou's Lemma),
$\int |\delta - \delta^k_{i,j}|^2 d\xi = \int \lim\limits_{k\to\infty} |\delta^{n_k}_{i,j} - \delta^k_{i,j}|^2 d\xi < \epsilon^2 < \infty$.

Thus, $\delta - \delta^k_{i,j} \in L_p(\mathbb{R})$ and $\delta = \delta - \delta^k_{i,j} + \delta^k_{i,j} \in L_p(\mathbb{R})$ with $\lim\limits_{n\to\infty} ||\delta - \delta^k_{i,j}||_2 = 0$.

Thus δ is limit in $L_2(\mathbb{R})$ of sequence $\{\delta^k_{i,j}\}$. Hence $L_p(\mathbb{R})$ is complete. □

Theorem 3.3. *[21] Let us assume that $f(\xi) = \frac{d^n u(\xi)}{d\xi^n} \in L^2(\mathbb{R})$ is a continuous function on [0,1] and its first derivative is bounded for all $\xi \in [0,1]$, $n \geq 2$. Then, the Fibonacci wavelet method will be convergent based on the approach proposed in [42]. That is, $|E_M|$ vanishes as J goes to infinity. The convergence is of order two [43] as follows $||E_M||_2 = O\Big[\Big(\frac{1}{2^{J+1}}\Big)^2\Big]$.*

3.1. Solution at collocation points

Let μ be a set of all collocation points which is measurable. Let $\{C_i\}$ be the sequence of collocation points and $\{f_i^k\}$ be the sequence of functional values at $\{C_i\}$ that satisfies the given system of differential equations. Here f^k is a function from $\mathbb{Z}^+$ to $\mathbb{R}$ defined by $f^k(i) = f_i^k$. Then,

$$f^k(\xi) = \sum_{i=1}^{\infty} f^k(i),$$

where $f^k(\xi)$ is an exact solution of a given system of k-differential equations.

4. Operational matrix of integration (OMI)

The Fibonacci wavelet basis at $k = 1$ and $M = 10$ is investigated as follows [44]:

$$\begin{aligned}
\delta_{1,0}(\xi) =& 1,\\
\delta_{1,1}(\xi) =& \sqrt{3}\xi,\\
\delta_{1,2}(\xi) =& \frac{1}{2}\sqrt{\frac{15}{7}}(1+\xi^2),\\
\delta_{1,3}(\xi) =& \sqrt{\frac{105}{239}}\,\xi\,(2+\xi^2),\\
\delta_{1,4}(\xi) =& 3\sqrt{\frac{35}{1943}}\,(1+3\xi^2+\xi^4),\\
\delta_{1,5}(\xi) =& \frac{3}{4}\sqrt{\frac{385}{2582}}\,\xi\,(3+4\xi^2+\xi^4),\\
\delta_{1,6}(\xi) =& 3\sqrt{\frac{5005}{1268209}}\,(1+6\xi^2+5\xi^4+\xi^6),\\
\delta_{1,7}(\xi) =& 3\sqrt{\frac{5005}{2827883}}\,\xi\,(4+10\xi^2+15\xi^4+7\xi^6+\xi^8),\\
\delta_{1,8}(\xi) =& \frac{3}{2}\sqrt{\frac{85085}{28195421}}\,(1+10\xi^2+15\xi^4+7\xi^6+\xi^8),\\
\delta_{1,9}(\xi) =& 3\sqrt{\frac{1616615}{5016284989}}\,\xi\,(5+20\xi^2+21\xi^4+8\xi^6+\xi^8).
\end{aligned}$$

Let

$$\begin{aligned}
&\delta_{10}(x)\\
=&[\delta_{1,0}(\xi), \delta_{1,1}(\xi), \delta_{1,2}(\xi), \delta_{1,3}(\xi), \delta_{1,4}(\xi), \delta_{1,5}(\xi), \delta_{1,6}(\xi), \delta_{1,7}(\xi), \delta_{1,8}(\xi), \delta_{1,9}(\xi)]^T.
\end{aligned}$$

As a linear combination of Fibonacci wavelet basis, integrate the first ten basis mentioned above for the range of ξ limits from 0 to ξ. We acquire, as

$$\int_0^{\xi} \delta_{1,0}(\xi)d\xi = \begin{bmatrix} 0 & \frac{1}{\sqrt{3}} & 0 & 0 & 0 & 0 & 0 & 0 & 0 & 0 \end{bmatrix} \delta_{10}(\xi),$$
$$\int_0^{\xi} \delta_{1,1}(\xi)d\xi = \begin{bmatrix} -\frac{\sqrt{3}}{2} & 0 & \sqrt{\frac{7}{5}} & 0 & 0 & 0 & 0 & 0 & 0 & 0 \end{bmatrix} \delta_{10}(\xi),$$

$$\int_0^{\xi} \delta_{1,2}(\xi)d\xi = \begin{bmatrix} 0 & \frac{\sqrt{5}}{6\sqrt{7}} & 0 & \frac{\sqrt{239}}{42} & 0 & 0 & 0 & 0 & 0 & 0 \end{bmatrix} \delta_{10}(\xi),$$

$$\int_0^{\xi} \delta_{1,3}(\xi)d\xi = \begin{bmatrix} -\frac{\sqrt{105}}{2\sqrt{239}} & 0 & \frac{7}{2\sqrt{239}} & 0 & \frac{\sqrt{1943}}{4\sqrt{717}} & 0 & 0 & 0 & 0 & 0 \end{bmatrix} \delta_{10}(\xi),$$

$$\int_0^{\xi} \delta_{1,4}(\xi)d\xi = \begin{bmatrix} 0 & 0 & 0 & \frac{\sqrt{717}}{5\sqrt{1943}} & 0 & \frac{4\sqrt{2582}}{5\sqrt{21373}} & 0 & 0 & 0 & 0 \end{bmatrix} \delta_{10}(\xi),$$

$$\int_0^{\xi} \delta_{1,5}(\xi)d\xi = \begin{bmatrix} -\frac{\sqrt{385}}{4\sqrt{2582}} & 0 & 0 & 0 & \frac{\sqrt{21373}}{24\sqrt{2582}} & 0 & \frac{\sqrt{1268209}}{24\sqrt{33566}} & 0 & 0 & 0 \end{bmatrix} \delta_{10}(\xi),$$

$$\int_0^{\xi} \delta_{1,6}(\xi)d\xi = \begin{bmatrix} 0 & 0 & 0 & 0 & 0 & \frac{4\sqrt{33566}}{7\sqrt{1268209}} & 0 & \frac{\sqrt{2827883}}{7\sqrt{1268209}} & 0 & 0 \end{bmatrix} \delta_{10}(\xi),$$

$$\int_0^{\xi} \delta_{1,7}(\xi)d\xi = \begin{bmatrix} -\frac{3\sqrt{5005}}{4\sqrt{2827883}} & 0 & 0 & 0 & 0 & 0 & \frac{\sqrt{1268209}}{8\sqrt{2827883}} & 0 & \frac{\sqrt{28195421}}{4\sqrt{48074011}} & 0 \end{bmatrix} \delta_{10}(\xi),$$

$$\int_0^{\xi} \delta_{1,8}(\xi)d\xi = \begin{bmatrix} 0 & 0 & 0 & 0 & 0 & 0 & 0 & \frac{\sqrt{48074011}}{18\sqrt{28195421}} & 0 & \frac{\sqrt{5016284989}}{18\sqrt{535712999}} \end{bmatrix} \delta_{10}(\xi),$$

$$\int_0^{\xi} \delta_{1,9}(\xi)d\xi = \begin{bmatrix} -3\sqrt{\frac{323323}{25081424945}} & 0 & 0 & 0 & 0 & 0 & 0 & 0 & \frac{\sqrt{535712999}}{5\sqrt{5016284989}} & 0 \end{bmatrix} \delta_{10}(\xi) + \frac{\sqrt{11941544471}}{10\sqrt{5016284989}} \delta_{1,10}(\xi).$$

Hence,

$$\int_0^{\xi} \delta(\xi)d\xi = \Phi_{10\times 10}\ \delta_{10}(\xi) + \overline{\delta_{10}(\xi)}, \tag{4.1}$$

where

$$\Phi_{10\times 10} = \begin{bmatrix}
0 & \frac{1}{\sqrt{3}} & 0 & 0 & 0 & 0 & 0 & 0 & 0 & 0 \\
-\frac{\sqrt{3}}{2} & 0 & \sqrt{\frac{7}{5}} & 0 & 0 & 0 & 0 & 0 & 0 & 0 \\
0 & \frac{\sqrt{5}}{6\sqrt{7}} & 0 & \frac{\sqrt{239}}{42} & 0 & 0 & 0 & 0 & 0 & 0 \\
-\frac{\sqrt{105}}{2\sqrt{239}} & 0 & \frac{7}{2\sqrt{239}} & 0 & \frac{\sqrt{1943}}{4\sqrt{717}} & 0 & 0 & 0 & 0 & 0 \\
0 & 0 & 0 & \frac{\sqrt{717}}{5\sqrt{1943}} & 0 & \frac{4\sqrt{2582}}{5\sqrt{21373}} & 0 & 0 & 0 & 0 \\
-\frac{\sqrt{385}}{4\sqrt{2582}} & 0 & 0 & 0 & \frac{\sqrt{21373}}{24\sqrt{2582}} & 0 & \frac{\sqrt{1268209}}{24\sqrt{33566}} & 0 & 0 & 0 \\
-\frac{3\sqrt{5005}}{4\sqrt{2827883}} & 0 & 0 & 0 & 0 & 0 & \frac{\sqrt{1268209}}{8\sqrt{2827883}} & 0 & \frac{\sqrt{28195421}}{4\sqrt{48074011}} & 0 \\
0 & 0 & 0 & 0 & 0 & 0 & 0 & \frac{\sqrt{48074011}}{18\sqrt{28195421}} & 0 & \frac{\sqrt{5016284989}}{18\sqrt{535712999}} \\
-3\sqrt{\frac{323323}{25081424945}} & 0 & 0 & 0 & 0 & 0 & 0 & 0 & \frac{\sqrt{535712999}}{5\sqrt{5016284989}} & 0
\end{bmatrix},$$

$$\overline{\delta_{10}(\xi)} = \begin{bmatrix} 0 \\ 0 \\ 0 \\ 0 \\ 0 \\ 0 \\ 0 \\ 0 \\ 0 \\ \frac{\sqrt{11941544471}}{10\sqrt{5016284989}}\delta_{1,10}(\xi) \end{bmatrix}.$$

Again, integrating the above ten bases, we obtain,

$$\int_0^\xi\int_0^\xi \delta_{1,0}(\xi)d\xi d\xi = \begin{bmatrix} \frac{1}{2} & 0 & \sqrt{\frac{7}{15}} & 0 & 0 & 0 & 0 & 0 & 0 & 0 \end{bmatrix}\delta_{10}(\xi),$$

$$\int_0^\xi\int_0^\xi \delta_{1,1}(\xi)d\xi d\xi = \begin{bmatrix} 0 & -\frac{1}{3} & 0 & \frac{\sqrt{239}}{6\sqrt{35}} & 0 & 0 & 0 & 0 & 0 & 0 \end{bmatrix}\delta_{10}(\xi),$$

$$\int_0^\xi\int_0^\xi \delta_{1,2}(\xi)d\xi d\xi = \begin{bmatrix} -\frac{\sqrt{5}}{2\sqrt{21}} & 0 & \frac{1}{4} & 0 & \frac{\sqrt{1943}}{168\sqrt{3}} & 0 & 0 & 0 & 0 & 0 \end{bmatrix}\delta_{10}(\xi),$$

$$\int_0^\xi\int_0^\xi \delta_{1,3}(\xi)d\xi d\xi = \begin{bmatrix} 0 & -\frac{5\sqrt{35}}{12\sqrt{239}} & 0 & \frac{2}{15} & 0 & \frac{\sqrt{2582}}{5\sqrt{7887}} & 0 & 0 & 0 & 0 \end{bmatrix}\delta_{10}(\xi),$$

$$\int_0^\xi\int_0^\xi \delta_{1,4}(\xi)d\xi d\xi = \begin{bmatrix} -\frac{\sqrt{35}}{2\sqrt{1943}} & 0 & \frac{7\sqrt{3}}{10\sqrt{1943}} & 0 & \frac{1}{12} & 0 & \frac{\sqrt{1268209}}{30\sqrt{277849}} & 0 & 0 & 0 \end{bmatrix}\delta_{10}(\xi),$$

$$\int_0^\xi\int_0^\xi \delta_{1,5}(\xi)d\xi d\xi = \begin{bmatrix} 0 & -\frac{\sqrt{385}}{4\sqrt{7746}} & 0 & \frac{\sqrt{2629}}{40\sqrt{7746}} & 0 & \frac{2}{35} & 0 & \frac{\sqrt{2827883}}{168\sqrt{33566}} & 0 & 0 \end{bmatrix}\delta_{10}(\xi),$$

$$\int_0^\xi\int_0^\xi \delta_{1,6}(\xi)d\xi d\xi = \begin{bmatrix} -\frac{\sqrt{5005}}{4\sqrt{1268209}} & 0 & 0 & 0 & \frac{\sqrt{277849}}{42\sqrt{1268209}} & 0 & \frac{1}{24} & 0 & \frac{\sqrt{28195421}}{28\sqrt{21559553}} & 0 \end{bmatrix} \delta_{10}(\xi),$$

$$\int_0^\xi\int_0^\xi \delta_{1,7}(\xi)d\xi d\xi = \begin{bmatrix} 0 & -\frac{\sqrt{15015}}{4\sqrt{2827883}} & 0 & 0 & 0 & \frac{\sqrt{16783}}{7\sqrt{5655766}} & 0 & \frac{2}{63} & 0 & \frac{\sqrt{5016284989}}{72\sqrt{913406209}} \end{bmatrix} \delta_{10}(\xi),$$

$$\int_0^\xi\int_0^\xi \delta_{1,8}(\xi)d\xi d\xi = \begin{bmatrix} -\frac{3\sqrt{17017}}{8\sqrt{140977105}} & 0 & 0 & 0 & 0 & 0 & \frac{\sqrt{21559553}}{144\sqrt{28195421}} & 0 & \frac{1}{40} & 0 \end{bmatrix}\delta_{10}(\xi)$$

$$+ \frac{\sqrt{11941544471}}{180\sqrt{535712999}}\delta_{1,10}(\xi),$$

$$\int_0^\xi \int_0^\xi \delta_{1,9}(\xi) d\xi d\xi = \begin{bmatrix} 0 & -\sqrt{\frac{969969}{25081424945}} & 0 & 0 & 0 & 0 & 0 & \frac{\sqrt{913406209}}{90\sqrt{5016284989}} & 0 & \frac{2}{99} \end{bmatrix} \delta_{10}(\xi) + \frac{4\sqrt{10276002038}}{55\sqrt{115374554747}}\delta_{1,11}(\xi).$$

Hence,

$$\int_0^\xi \int_0^\xi \delta(\xi) d\xi d\xi = \Phi'_{10\times 10}\ \delta(\xi) + \overline{\delta'_{10}(\xi)}. \tag{4.2}$$

$$\Phi'_{10\times10} = \begin{bmatrix}
-\frac{1}{2} & 0 & \sqrt{\frac{7}{15}} & 0 & 0 & 0 & 0 & 0 & 0 & 0 \\
0 & -\frac{1}{3} & 0 & \frac{\sqrt{239}}{6\sqrt{35}} & 0 & 0 & 0 & 0 & 0 & 0 \\
-\frac{\sqrt{5}}{2\sqrt{21}} & 0 & \frac{1}{4} & 0 & \frac{\sqrt{1943}}{168\sqrt{3}} & 0 & 0 & 0 & 0 & 0 \\
0 & -\frac{5\sqrt{35}}{12\sqrt{239}} & 0 & \frac{2}{15} & 0 & \frac{\sqrt{2582}}{5\sqrt{7887}} & 0 & 0 & 0 & 0 \\
-\frac{\sqrt{35}}{2\sqrt{1943}} & 0 & \frac{7\sqrt{3}}{10\sqrt{1943}} & 0 & \frac{1}{12} & 0 & \frac{\sqrt{1268209}}{30\sqrt{277849}} & 0 & 0 & 0 \\
0 & -\frac{\sqrt{385}}{4\sqrt{7746}} & 0 & \frac{\sqrt{2629}}{40\sqrt{7746}} & 0 & \frac{2}{35} & 0 & \frac{\sqrt{2827883}}{168\sqrt{33566}} & 0 & 0 \\
-\frac{\sqrt{5005}}{4\sqrt{1268209}} & 0 & 0 & 0 & \frac{\sqrt{277849}}{42\sqrt{1268209}} & 0 & \frac{1}{24} & 0 & \frac{\sqrt{28195421}}{28\sqrt{215559553}} & 0 \\
0 & -\frac{\sqrt{15015}}{4\sqrt{2827883}} & 0 & 0 & 0 & \frac{\sqrt{116783}}{7\sqrt{5655766}} & 0 & \frac{2}{63} & 0 & \frac{\sqrt{5016284989}}{72\sqrt{913406209}} \\
-\frac{3\sqrt{17017}}{8\sqrt{140977105}} & 0 & 0 & 0 & 0 & 0 & \frac{\sqrt{21559553}}{144\sqrt{28195421}} & 0 & \frac{1}{0} & 0 \\
0 & -\sqrt{\frac{969969}{25081424945}} & 0 & 0 & 0 & 0 & 0 & \frac{\sqrt{913406209}}{90\sqrt{5016284989}} & 0 & \frac{2}{99}
\end{bmatrix},$$

$$\overline{\delta'_{10}(\xi)} = \begin{bmatrix} 0 \\ 0 \\ 0 \\ 0 \\ 0 \\ 0 \\ 0 \\ 0 \\ \frac{\sqrt{11941544471}}{180\sqrt{535712999}}\delta_{1,10}(\xi) \\ \frac{4\sqrt{10276002038}}{55\sqrt{115374554747}}\delta_{1,11}(\xi) \end{bmatrix}.$$

We may also create the operational matrix for our convenience at various sizes in the same manner.

5. Fibonacci wavelet method

Generalized form of (1.1) is

$$\mathscr{Z}_p^{''}(\xi) = \alpha_p \mathscr{Z}_p(\xi) + f_p(\xi, \mathscr{Z}_1(\xi), \ldots, \mathscr{Z}_p(\xi), \mathscr{Z}_1^{'}(\xi), \ldots, \mathscr{Z}_p^{'}(\xi), \mathscr{Z}_1(q\xi), \ldots, \mathscr{Z}_p(q_p\xi)), \tag{5.1}$$

where $1 \leq p \leq n$ with the initial conditions $\mathscr{Z}_p(0) = \beta_p$, $\mathscr{Z}_p^{'}(0) = \gamma_p$ and q_p represents delay terms. Assume that

$$\mathscr{Z}_p^{''}(\xi) = \sum_{r=1}^{\infty}\sum_{s=0}^{\infty} a_{r,s}^p\, \delta_{r,s}(\xi) = \sum_{i=1}^{\infty} a_i^p \delta(\xi),\ 1 \leq p \leq n.$$

Truncating the above equation we get,

$$\mathscr{Z}_p^{''}(\xi) = \sum_{r=1}^{2^{k-1}}\sum_{s=0}^{M-1} a_{r,s}^p\, \delta_{r,s}(\xi) = \sum_{i=1}^{2^{k-1}M} a_i^p \delta(\xi) = A^T\delta(\xi),\ 1 \leq p \leq n, \tag{5.2}$$

where, $\delta_{r,s} = \delta(\xi) = \left[\delta_{1,0}, \ldots, \delta_{1,M-1}, \delta_{2,1}, \ldots, \delta_{2,M-1}, \ldots, \delta_{2^{k-1},0}, \ldots, \delta_{2^{k-1},M-1}\right]^T$ and $a_{r,s}^p = a_i^p = \left[a_1^p, a_2^p, \ldots, a_{2^{k-1}M}^p\right]$. Integrating (5.2) with respect to ξ limit from 0 to ξ, we obtain,

$$\begin{aligned} \mathscr{Z}_p^{'}(\xi) &= \mathscr{Z}_p^{'}(0) + A^T[\Phi\delta(\xi) + \overline{\delta_{10}(\xi)}], \\ \mathscr{Z}_p^{'}(\xi) &= \gamma_p + A^T[\Phi\delta(\xi) + \overline{\delta_{10}(\xi)}], \end{aligned} \tag{5.3}$$

where A^T is the unknown coefficient matrix and Φ and $\overline{\delta_{10}(\xi)}$ are the operational matrices obtained in section 3.

Integrate (5.3) with respect to ξ limit from 0 to ξ, we obtain

$$\begin{aligned} \mathscr{Z}_p(\xi) &= \mathscr{Z}_p(0) + \xi\gamma_p + A^T[\Phi^{'}\delta(\xi) + \overline{\delta_{10}^{'}(\xi)}], \\ \mathscr{Z}_p(\xi) &= \beta_p + +\xi\gamma_p + A^T[\Phi^{'}\delta(\xi) + \overline{\delta_{10}^{'}(\xi)}]. \end{aligned} \tag{5.4}$$

Fit (5.4), (5.3) and (5.2) into (5.1) for each fixed value of $p = 1, ..., n$. Then collocate the obtained equation using the following grid points:

$$\xi_i = \frac{2i-1}{2^k M}, i = 1, ..., 2^{k-1}M.$$

Then we obtain the following system algebraic equations

$$\left.\begin{aligned} &F_1(a_1^1, a_2^1, ..., a_{2^{k-1}M}^1, a_1^2, a_2^2, ..., a_{2^{k-1}M}^2, ..., a_1^n, a_2^n, ..., a_{2^{k-1}M}^n) = 0, \\ &F_2(a_1^1, a_2^1, ..., a_{2^{k-1}M}^1, a_1^2, a_2^2, ..., a_{2^{k-1}M}^2, ..., a_1^n, a_2^n, ..., a_{2^{k-1}M}^n) = 0, \\ &\qquad\vdots \\ &F_{n\times 2^{k-1}M}(a_1^1, a_2^1, ..., a_{2^{k-1}M}^1, a_1^2, a_2^2, ..., a_{2^{k-1}M}^2, ..., a_1^n, a_2^n, ..., a_{2^{k-1}M}^n) = 0. \end{aligned}\right\} \tag{5.5}$$

To find the values of unknown Fibonacci wavelet coefficients a_i^k, where $i = 1, ...,$ $2^{k-1}M$ and $k = 1, ..., n$, we considered the Newton-Raphson method as follows: If the initial guess of the root is a_i^k and a_{i+1}^k is the point at which the slope intercepts, then the Taylor series expansion of (5.5) can be written as

$$F_{1,i+1} = F_{1,i} + (a_{1,i+1}^k - a_{1,i}^k)\frac{\partial F_{1,i}}{\partial a_1^k} + (a_{2,i+1}^k - a_{2,i}^k)\frac{\partial F_{1,i}}{\partial a_2^k} +, ..., + (a_{2^{k-1}M,i+1}^k - a_{2^{k-1}M,i}^k) \frac{\partial F_{1,i}}{\partial a_{2^{k-1}M}^k}, \tag{5.6}$$

where $k = 1, 2, 3, ..., n$. Applying the Taylor expansion similarly for $F_2, F_3, F_4, ...,$ $F_{n\times 2^{k-1}M}$, and generalizing for $n \times 2^{k-1}M$ equations, we get,

$$\begin{aligned} &\frac{\partial F_{k,i}}{\partial a_1^k} a_{1,i+1}^k + \frac{\partial F_{k,i}}{\partial a_2^k} a_{2,i+1}^k +, ..., + \frac{\partial F_{k,i}}{\partial a_{2M}^k} a_{2M,i+1}^k \\ =& - F_{k,i} + a_{1,i}^k \frac{\partial F_{k,i}}{\partial a_1^k} + a_{2,i}^k \frac{\partial F_{k,i}}{\partial a_2^k} +, ..., \\ &+ a_{2^{k-1}M,i}^k \frac{\partial F_{k,i}}{\partial a_{2^{k-1}M}^k}, \end{aligned} \tag{5.7}$$

where the first subscript k represents the equations in (5.5), and the second subscript denotes the function value at the present value (i) or at the next value $(i+1)$. (5.7) can be represented in a matrix notation as:

$$[J][a_{i+1}^k] = -[F] + [J][a_i^k], \tag{5.8}$$

where the partial derivatives evaluated at i are written as the Jacobian matrix consisting of partial derivatives:

$$[J] = \begin{bmatrix} \frac{\partial F_{1,i}}{\partial a_1^k} & \frac{\partial F_{1,i}}{\partial a_2^k} & \cdots & \frac{\partial F_{1,i}}{\partial a_{2^{k-1}M}^k} \\ \frac{\partial F_{2,i}}{\partial a_1^k} & \frac{\partial F_{2,i}}{\partial a_2^k} & \cdots & \frac{\partial F_{2,i}}{\partial a_{2^{k-1}M}^k} \\ \vdots & & \cdots & \vdots \\ \frac{\partial F_{n,i}}{\partial a_1^k} & \frac{\partial F_{n,i}}{\partial a_2^k} & \cdots & \frac{\partial F_{n,i}}{\partial a_{2^{k-1}M}^k} \end{bmatrix}.$$

The initial and final values are expressed in the vector form as:

$[a_i^k]^T = \begin{bmatrix} a_{1,i}^k & a_{2,i}^k & \cdots & a_{n,i}^k \end{bmatrix}$, $[a_{i+1}^k]^T = \begin{bmatrix} a_{1,i+1}^k & a_{2,i+1}^k & \cdots & a_{n,i+1}^k \end{bmatrix}$, and $[F]^T = \begin{bmatrix} F_{1,i} & F_{2,i} & \cdots & F_{n,i} \end{bmatrix}$.

Multiplying the inverse of the Jacobian to (5.8)

$$[a_{i+1}^k] = [a_i^k] - [J]^{-1}[F]. \tag{5.9}$$

From (5.9), we get the unknown Fibonacci wavelet coefficients $a_i^k s$. Using $a_i^k s$ in equation (5.4), we get the desired solution of the considered system (1.1).

6. Numerical illustration

Here, we employ the FWCM to solve a Pantograph-type equation. We find a suitable solution for the considered equations using the operational integration matrix via the FWCM. Then, we transform the nonlinear differential equations into a set of algebraic equations. Later, with the Newton-Raphson approach, the set of nonlinear algebraic equations is resolved, and the Fibonacci wavelet coefficients and wavelet-based numerical solutions of Pantograph equations are obtained by substituting these coefficient values.

Problem 1. Consider the second-order nonlinear system of Pantograph-type equations. [4]

$$\left.\begin{array}{l}\mathscr{X}_1''(\xi)+\mathscr{X}_1'(\xi)-\xi\mathscr{X}_2'(\xi)+\mathscr{X}_1(\xi)+\mathscr{X}_1(\xi)\mathscr{X}_2(\xi)+\mathscr{X}_1(\xi)\mathscr{X}_2(\frac{\xi}{2})=\frac{3\xi^3}{2}-3\xi^2-\frac{7\xi}{2}+11,\\ -\xi\mathscr{X}_1''(\xi)+\mathscr{X}_2'(\xi)+\mathscr{X}_1(\xi)+\mathscr{X}_1^2(\xi)+\mathscr{X}_2^2(\frac{\xi}{5})=\xi^4-\frac{126\xi^2}{25}+\frac{14\xi}{5}+3.\end{array}\right\} \tag{6.1}$$

With initial conditions

$$\mathscr{X}_1(0)=-3,\ \mathscr{X}_2(0)=-3,\ \mathscr{X}_1'(0)=0. \tag{6.2}$$

The exact solutions are: $\mathscr{X}_1(\xi)=\xi^2-3$, $\mathscr{X}_2(\xi)=\xi-2$. The FWCM solutions for problem 1 are shown in Figures 1 and 2, revealing that the proposed method yields the exact solution. It can be seen from Figures 1 and 2 that the solutions are stable and tend to the specified function (which can be a solution for the equation physically). These figures show minimal changes in approximate solutions with and without noises. So, our approximate method is numerically stable. The exact solution and numerical approximations produced by the implemented FWCM approach are compared and tabulated in Table 1. Figures 1 and 2 depict all the graphical representations of numerical simulations.

Table 1. Numerical comparison for $\mathscr{X}_1(\xi)$ and $\mathscr{X}_2(\xi)$ with the eaxct solution of Problem 1.

$\mathscr{X}_1(\xi)$			$\mathscr{X}_2(\xi)$		
ξ	Exact Solution	FWCM Solution	ξ	Exact Solution	FWCM Solution
0	-3.00	-3.00	0	-2.0	-2.0
0.1	-2.99	-2.99	0.1	-1.9	-1.9
0.2	-2.96	-2.96	0.2	-1.8	-1.8
0.3	-2.91	-2.91	0.3	-1.7	-1.7
0.4	-2.84	-2.84	0.4	-1.6	-1.6
0.5	-2.75	-2.75	0.5	-1.5	-1.5
0.6	-2.64	-2.64	0.6	-1.4	-1.4
0.7	-2.51	-2.51	0.7	-1.3	-1.3
0.8	-2.36	-2.36	0.8	-1.2	-1.2
0.9	-2.19	-2.19	0.9	-1.1	-1.1
1.0	-2.00	-2.00	1.0	-1.0	-1.0

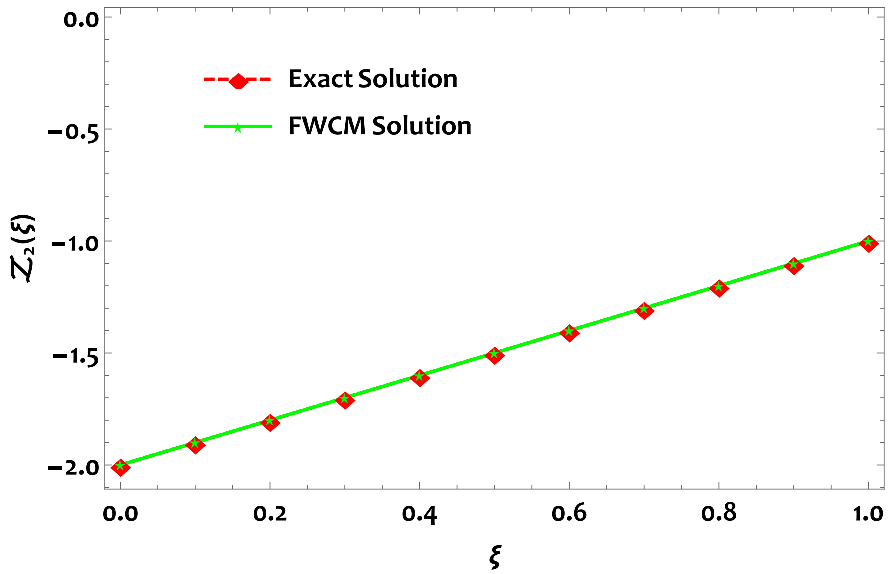

Figure 2. Graphical comparision of the FWCM solution $\mathscr{Z}_2(\xi)$ for Problem 1.

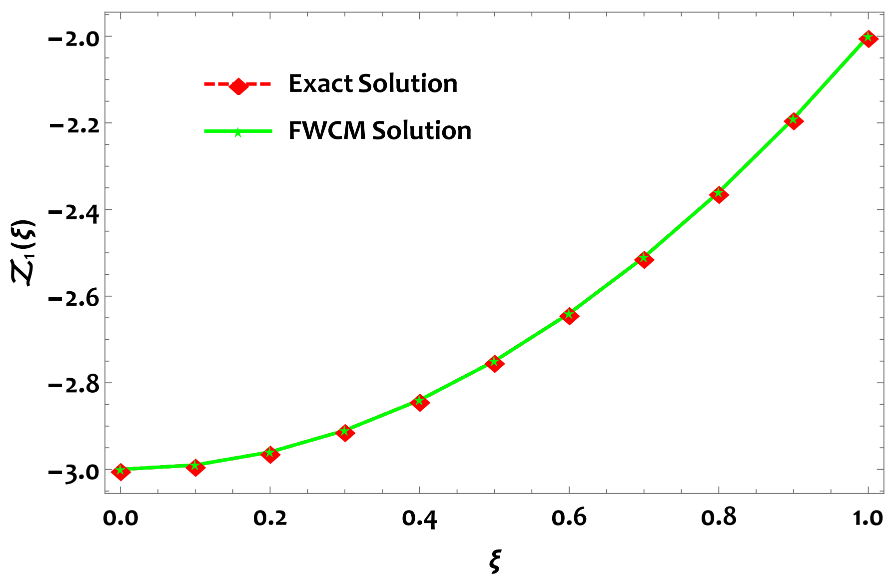

Figure 1. Graphical comparision of the FWCM solution $\mathscr{Z}_1(\xi)$ for Problem 1.

Problem 2: Consider the following system of a Pantograph type equation [4]

$$\left.\begin{aligned} -\mathscr{Z}_1''(\xi) + \mathscr{Z}_2''(\xi) + \xi\mathscr{Z}_1'(\xi) + \mathscr{Z}_1(\tfrac{\xi}{2})\mathscr{Z}_2(\tfrac{\xi}{2}) = g_1(\xi),\\ \xi\mathscr{Z}_2''(\xi) + \mathscr{Z}_1''(\xi) + \mathscr{Z}_2^2(\xi) + \mathscr{Z}_2(\tfrac{\xi}{2})\mathscr{Z}_1(\tfrac{\xi}{10}) = g_2(\xi). \end{aligned}\right\} \tag{6.3}$$

With initial conditions,

$$\mathscr{Z}_1'(0) = 1,\ \mathscr{Z}_2(0) = 0,\ \mathscr{Z}_1'(0) = 2\ \mathscr{Z}_2'(0) = -2. \tag{6.4}$$

The exact solutions are

$$\mathscr{Z}_1(\xi) = e^{2\xi},\ \mathscr{Z}_2(\xi) = e^{-2\xi}.$$

Here, $g_1(\xi) = -2e^{2\xi}\xi + e^{\frac{3\xi}{5}} + 4e^{-2\xi}$, and $g_2(\xi) = 4e^{-2\xi}(\xi + e^{4\xi}) + 2e^{\frac{4\xi}{5}} + e^{-4\xi}$. The numerical and exact solutions are compared with FCM (Fibonacci collocation method) solutions, and the values are tabulated in Tables 2 and 3. The absolute error between the analytical and approximative solutions is presented in the same tables. Figures 3 and 4 provide the visual representation of the obtained solution by FWCM compared with the FCM solution. The graphical representation of the absolute error of our suggested approach is carried out in Figures 5 and 6. The present method has more accurate results than the other method. A much smaller number of collocation points is used in the present method. The maximum absolute error in this method is much less than in the other method. The tables and figures show that the suggested approach provides superior accuracy over the current numerical methods. The tables and graphs show that the proposed approach converges more rapidly with the exact solution than other methods, and the proposed method is a suitable and powerful tool to solve the desired Pantograph equation.

Table 2. Numerical comparison for $\mathscr{Z}_1(\xi)$ with different methods of Problem 2.

ξ	Exact Solution	FWCM Solution	AE of FWCM (k=1, M=8)	AE of FCM ($E_{\mathbf{1,8}}$)
0	1.00000000000	1.00000000000	0	0
0.1	1.22140275816	1.22140270375	5.44×10^{-8}	-
0.2	1.49182469764	1.49182459299	1.04×10^{-7}	9.80×10^{-8}
0.3	1.82211880039	1.82211864961	1.50×10^{-7}	-
0.4	2.22554092849	2.22554073328	1.92×10^{-7}	2.10×10^{-7}
0.5	2.71828182846	2.71828159234	2.36×10^{-7}	-
0.6	3.32011692274	3.32011664646	2.76×10^{-7}	3.25×10^{-7}
0.7	4.05519996684	4.05519965258	3.14×10^{-7}	-
0.8	4.95303242445	4.95303207109	3.53×10^{-7}	4.14×10^{-7}
0.9	6.04964746441	6.04964707292	3.91×10^{-7}	-
1.0	7.38905609893	7.38905567043	4.24×10^{-7}	1.54×10^{-5}

Table 3. Numerical comparison for $\mathscr{Z}_2(\xi)$ with different methods of Problem 2.

ξ	Exact Solution	FWCM Solution	AE of FWCM (k=1, M=8)	AE of FCM ($E_{\mathbf{1},\mathbf{8}}$)
0	1.00000000000	1.00000000000	0	0
0.1	0.81873075307	0.81873074490	8.17×10^{-9}	-
0.2	0.67032004603	0.67032003277	1.32×10^{-8}	2.75×10^{-8}
0.3	0.54881163609	0.54881162231	1.37×10^{-8}	-
0.4	0.44932896411	0.44932895468	9.43×10^{-9}	6.44×10^{-8}
0.5	0.36787944117	0.36787944136	1.91×10^{-10}	-
0.6	0.30119421191	0.30119422658	1.46×10^{-8}	1.12×10^{-7}
0.7	0.24659696394	0.24659699799	3.40×10^{-8}	-
0.8	0.20189651799	0.20189657572	5.77×10^{-8}	1.68×10^{-7}
0.9	0.16529888822	0.16529897414	8.59×10^{-8}	-
1.0	0.13533528323	0.13533540131	1.18×10^{-7}	2.60×10^{-6}

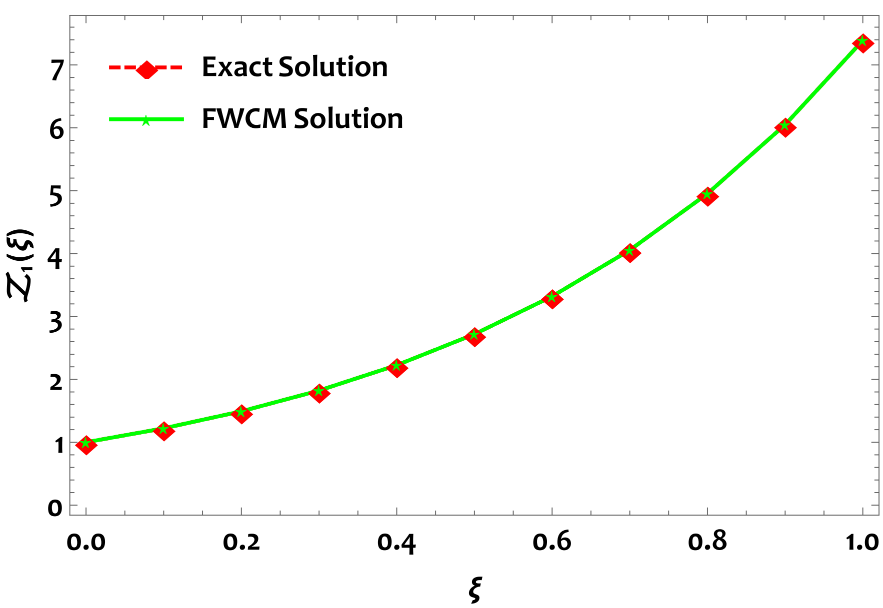

Figure 3. Graphical comparision of the FWCM solution $\mathscr{Z}_1(\xi)$ for Problem 2.

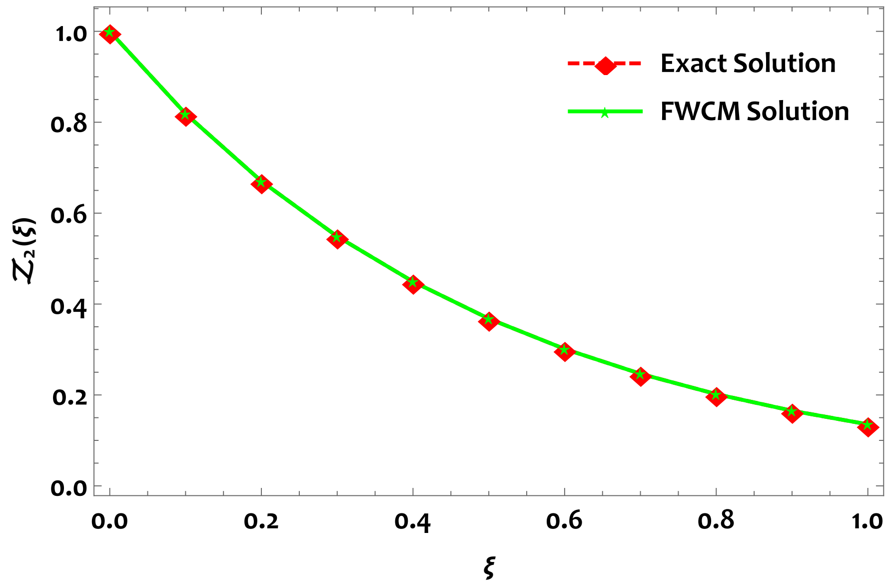

Figure 4. Graphical comparision of the FWCM solution $\mathscr{Z}_2(\xi)$ for Problem 2.

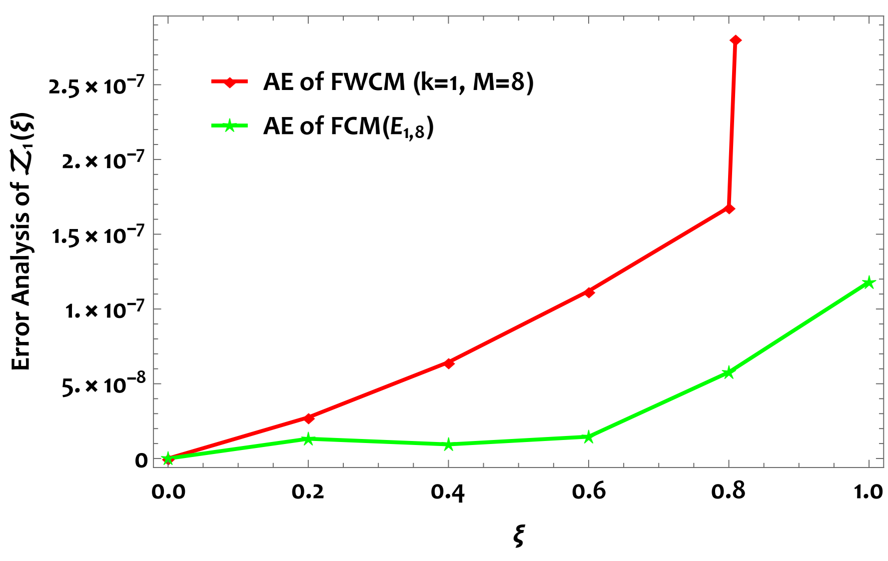

Figure 5. AE Comparison of FWCM and FCM solution with exact solution for Problem 2.

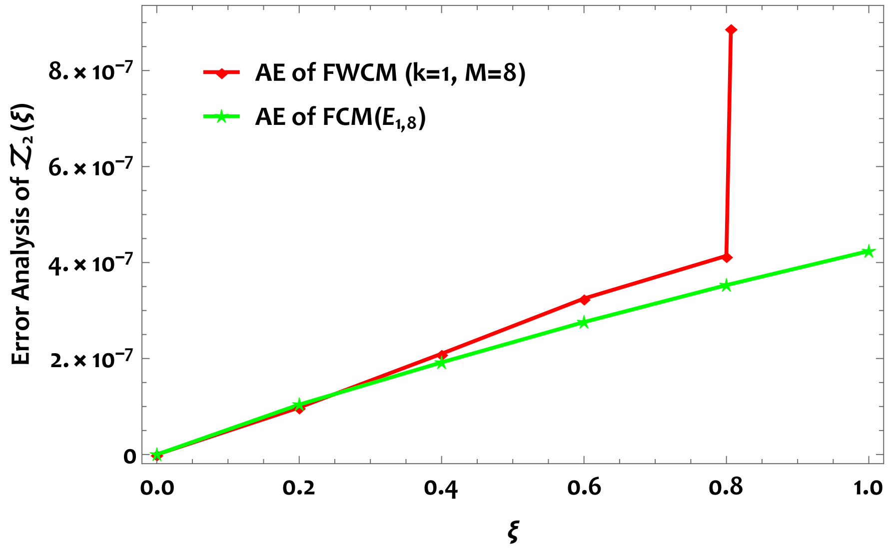

Figure 6. AE Comparison of FWCM and FCM solution with exact solution for Problem 2.

Problem 3: Consider the following system of a Pantograph type equation. [1]

$$\left.\begin{aligned} &-\mathscr{Z}_1'(\xi) + \mathscr{Z}_1(\xi) + e^{-\xi}\cos(\tfrac{\xi}{2})\mathscr{Z}_2(\tfrac{\xi}{2}) + 2e^{\frac{-3}{4\xi}}\cos(\tfrac{\xi}{2})\sin(\tfrac{\xi}{2})\mathscr{Z}_1(\tfrac{\xi}{4}) = 0,\\ &\mathscr{Z}_2'(\xi) - e^{x}\mathscr{Z}_1^2(\tfrac{\xi}{2}) + \mathscr{Z}_2^2(\tfrac{\xi}{2}) = 0. \end{aligned}\right\} \tag{6.5}$$

With initial conditions,

$$\mathscr{Z}_1(0) = 1,\ \mathscr{Z}_2(0) = 0, \tag{6.6}$$

and the exact solutions are

$$\mathscr{Z}_1(\xi) = e^{-\xi}\cos(\xi),\ \mathscr{Z}_2(\xi) = \sin(\xi).$$

The FWCM solutions for Problem 3 are shown in Tables 4-5 and Figures 7-8, revealing that the proposed method solutions are reasonably close to the exact solution compared to the current scheme, such as the Fibonacci collocation method (FCM) and Adomian decomposition method (ADM). Numerical approximations and absolute errors of the developed approach with the exact solution are tabulated in Tables 4-7. It is evident from Figures 7-8 that the approximations obtained from FWCM attain closer to the exact solution. The errors obtained using the proposed method are better than those obtained using other existing techniques. FWCM solutions are calculated at diverse values of M. Also, by increasing the values of M, we get more accuracy in the solution, which can be seen in Tables 6-7. It shows that increasing k and M can obtain a higher-order accuracy. Figures 9-10 depict all the graphical representations of numerical simulations and absolute error analysis. It can be seen that from Figures 1 and 2, the solutions are stable and tend to the specified function (which can be a solution for the equation physically). These figures show minimal changes in approximate solutions with and without noises. So, our approximate method is numerically stable.

Table 4. Numerical comparison for $\mathscr{X}_1(\xi)$ with different methods of Problem 3.

ξ	Exact Solution	FWCM Solution	AE of FWCM (k=1, M=8)	AE of ADM ($E_{\mathbf{1},\mathbf{3}}$)	AE of FCM ($E_{\mathbf{1},\mathbf{3}}$)
0	1.000000000000	1.000000000000	0	0	0
0.1	0.900316999845	0.900317002673	5.35×10^{-6}	-	-
0.2	0.802410647343	0.802410649338	3.23×10^{-6}	1.90×10^{-5}	9.36×10^{-4}
0.3	0.707730678026	0.707730679944	1.84×10^{-6}	-	-
0.4	0.617405647902	0.617405649481	1.99×10^{-6}	3.65×10^{-4}	1.01×10^{-3}
0.5	0.532280730216	0.532280731559	2.03×10^{-6}	-	-
0.6	0.452953789145	0.452953790266	1.08×10^{-6}	2.11×10^{-3}	1.97×10^{-4}
0.7	0.379809389925	0.379809390762	1.42×10^{-7}	-	-
0.8	0.313050504004	0.313050504826	9.65×10^{-7}	7.44×10^{-2}	8.46×10^{-4}
0.9	0.252727753291	0.252727753343	2.42×10^{-6}	-	-
1.0	0.198766110346	0.198766113439	5.66×10^{-6}	1.96×10^{-2}	1.06×10^{-2}

Table 5. Numerical comparison for $\mathscr{X}_2(\xi)$ with different methods of Problem 3.

ξ	Exact Solution	FWCM Solution	AE of FWCM (k=1, M=8)	AE of ADM ($E_{\mathbf{1},\mathbf{3}}$)	AE of FCM ($E_{\mathbf{1},\mathbf{3}}$)
0	1.000000000000	1.000000000000	0	0	0
0.1	0.099833416646	0.099833416886	1.85×10^{-6}	-	-
0.2	0.198669330795	0.198669331744	2.61×10^{-6}	1.67×10^{-5}	1.54×10^{-5}
0.3	0.295520206661	0.295520208145	3.47×10^{-6}	-	-
0.4	0.389418342309	0.389418344255	4.41×10^{-6}	1.79×10^{-4}	3.04×10^{-4}
0.5	0.479425538604	0.479425540985	5.06×10^{-6}	-	-
0.6	0.564642473395	0.564642476196	5.28×10^{-6}	3.28×10^{-4}	9.48×10^{-4}
0.7	0.644217687238	0.644217690425	5.38×10^{-6}	-	-
0.8	0.717356090952	0.717356094392	5.83×10^{-6}	1.27×10^{-3}	1.40×10^{-3}
0.9	0.783326909627	0.783326913406	6.44×10^{-6}	-	-
1.0	0.841470984808	0.841470988576	4.86×10^{-6}	1.01×10^{-2}	2.47×10^{-4}

Table 6. Comparision of $\mathscr{X}_1(\xi)$ with different values of M for Problem 3.

ξ	Exact Solution	AE of FWCM			
		k=1,M=3	k=2,M=3	k=1,M=5	k=1,M=5
0	1.000000000000	0	0	0	0
0.1	0.900316999845	5.35×10^{-6}	3.93×10^{-8}	2.82×10^{-9}	4.31×10^{-10}
0.2	0.802410647343	3.23×10^{-6}	3.09×10^{-8}	1.99×10^{-9}	2.32×10^{-10}
0.3	0.707730678026	1.84×10^{-6}	2.55×10^{-8}	1.91×10^{-9}	7.21×10^{-10}
0.4	0.617405647902	1.99×10^{-6}	2.64×10^{-8}	1.57×10^{-9}	3.82×10^{-10}
0.5	0.532280730216	2.03×10^{-6}	1.34×10^{-8}	1.34×10^{-9}	8.25×10^{-10}
0.6	0.452953789145	1.08×10^{-6}	3.04×10^{-7}	1.12×10^{-9}	2.82×10^{-10}
0.7	0.379809389925	1.42×10^{-7}	8.36×10^{-7}	8.36×10^{-10}	5.21×10^{-11}
0.8	0.313050504004	9.65×10^{-7}	1.48×10^{-6}	8.21×10^{-10}	6.28×10^{-11}
0.9	0.252727753291	2.42×10^{-6}	2.11×10^{-6}	5.18×10^{-11}	9.21×10^{-10}
1.0	0.198766110346	5.66×10^{-6}	2.54×10^{-6}	3.09×10^{-9}	3.62×10^{-10}

Table 7. Comparision of $\mathscr{X}_2(\xi)$ with different values of M for Problem 3.

ξ	Exact Solution	AE of FWCM			
		k=1,M=3	k=2,M=3	k=1,M=5	k=1,M=5
0	1.000000000000	0	0	0	0
0.1	0.099833416646	1.85×10^{-6}	1.62×10^{-8}	2.39×10^{-10}	4.31×10^{-10}
0.2	0.198669330795	2.61×10^{-6}	2.61×10^{-8}	9.38×10^{-10}	2.32×10^{-10}
0.3	0.295520206661	3.47×10^{-6}	3.28×10^{-8}	2.39×10^{-10}	7.21×10^{-10}
0.4	0.389418342309	4.41×10^{-6}	3.95×10^{-8}	2.39×10^{-10}	3.82×10^{-10}
0.5	0.479425538604	5.06×10^{-6}	2.38×10^{-9}	2.39×10^{-10}	8.25×10^{-10}
0.6	0.564642473395	5.28×10^{-6}	8.54×10^{-7}	2.39×10^{-10}	2.82×10^{-10}
0.7	0.644217687238	5.38×10^{-6}	1.33×10^{-5}	2.39×10^{-10}	5.21×10^{-11}
0.8	0.717356090952	5.83×10^{-6}	1.59×10^{-5}	2.39×10^{-10}	6.28×10^{-11}
0.9	0.783326909627	6.44×10^{-6}	1.70×10^{-5}	2.39×10^{-10}	9.21×10^{-10}
1.0	0.841470984808	4.86×10^{-6}	1.74×10^{-5}	2.39×10^{-10}	3.62×10^{-10}

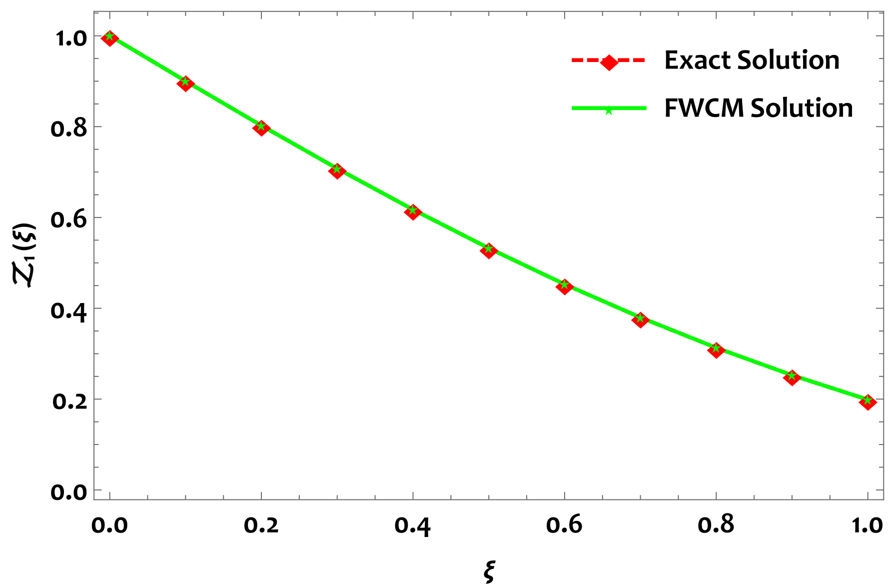

Figure 7. Graphical comparision of the FWCM solution $\mathscr{Z}_1(\xi)$ for Problem 3.

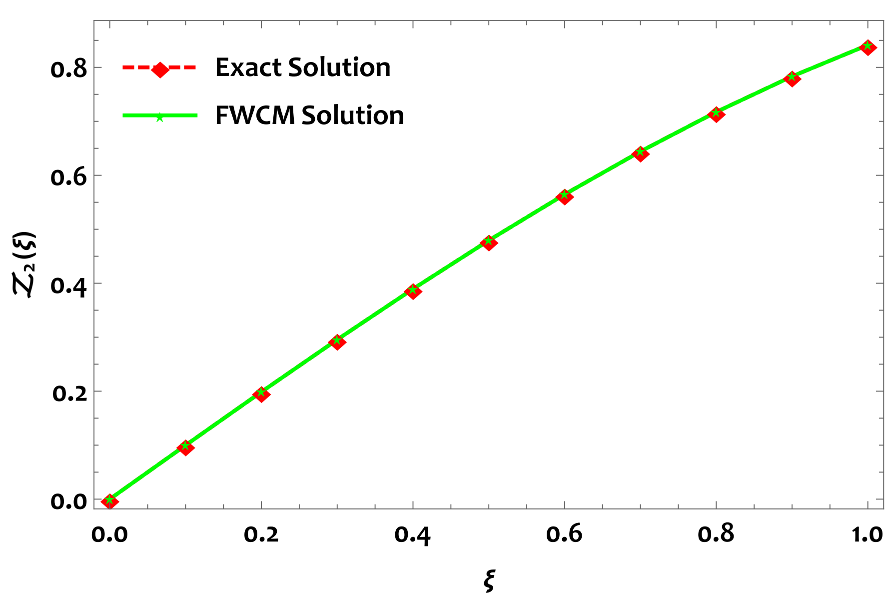

Figure 8. Graphical comparision of the FWCM solution $\mathscr{Z}_2(\xi)$ for Problem 3.

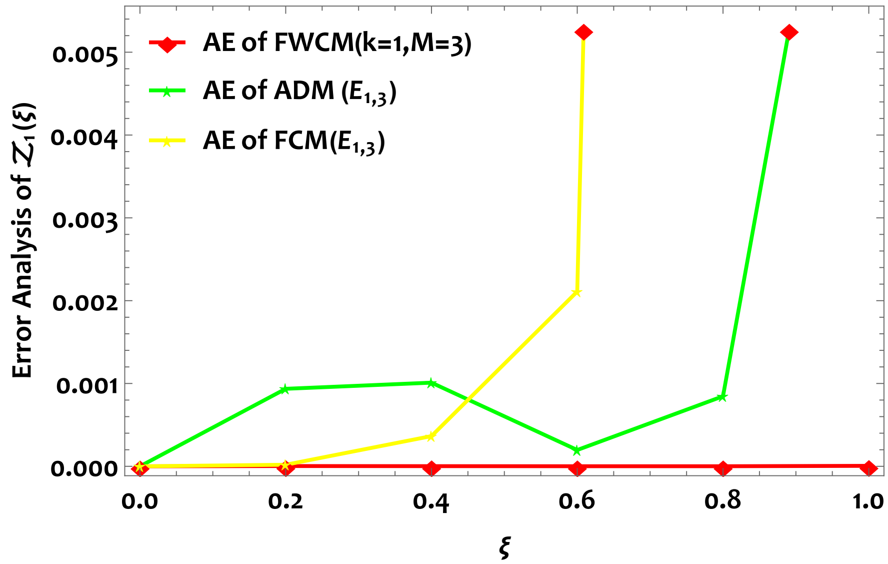

Figure 9. AE Comparison of FWCM, ADM and FCM solution with exact solution for Problem 3.

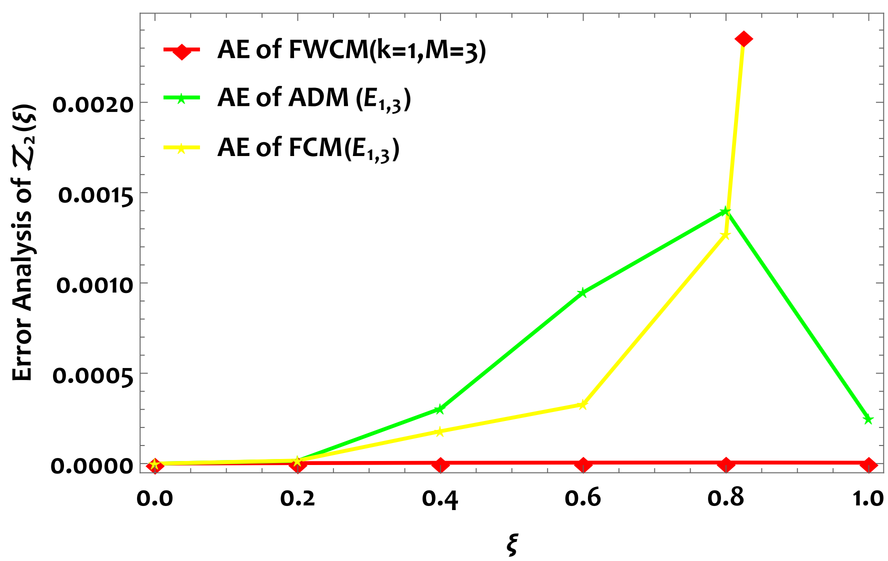

Figure 10. AE Comparison of FWCM, ADM and FCM solution with exact solution for Problem 3.

Problem 4: Consider the three-dimensional system of nonlinear pantograph delay differential equation: [1,8]

$$\left.\begin{aligned}\mathscr{X}_1'(\xi) &= \mathscr{X}_3(\xi) + 2\mathscr{X}_2(0.5\xi) + u_1(\xi),\\ \mathscr{X}_2'(\xi) &= -2\mathscr{X}_3^2(0.5\xi) + u_2(\xi),\\ \mathscr{X}_3'(\xi) &= -\mathscr{X}_1(\xi) + \mathscr{X}_2(\xi) + u_3(\xi).\end{aligned}\right\} \tag{6.7}$$

With the initial conditions,

$$\mathscr{X}_1(0) = -1,\ \mathscr{X}_2(0) = 0,\ \mathscr{X}_3(0) = 0. \tag{6.8}$$

The exact solutions are $\mathscr{X}_1(\xi) = \cos(\xi)$, $\mathscr{X}_2(\xi) = \xi\cos(\xi)$, $\mathscr{X}_1(\xi) = \sin(\xi)$. Here, $u_1(\xi) = -\xi\cos(\frac{\xi}{2})$, $u_2(\xi) = 1-\xi\sin(\xi)$, and $u_3(\xi) = -\xi\cos(\xi)$. Tables 8-10 provide the comparison of numerical approximations and absolute errors of the FWCM with the exact solution for $\mathscr{X}_1(\xi)$ and $\mathscr{X}_2(\xi)$. The absolute error between the exact and approximative solutions at different resolutions (various values of M) is presented in Tables 11-13. Figures 11-13 show a graphical illustration of the FWCM solution with the exact solution. Also, the graphical representation of the Absolute error (AE) of the proposed method with the FBP method is carried out in Figures 14-16. The absolute error between the analytical and approximative solutions at different resolutions (various M and k) is presented visually in Figures 17-19. Tables and graphs confirm that our proposed approach can generate more precise results by simply increasing the M and k values. The tables and figures show that the suggested approach provides superior accuracy over the current numerical methods.

Table 8. Numerical comparison for $\mathscr{X}_1(\xi)$ with FWCM of Problem 4.

ξ	Exact solution	$\lvert e_{1,4}(\xi)\rvert$		$\lvert e_{1,6}(\xi)\rvert$		$\lvert e_{1,9}(\xi)\rvert$	
		FWCM	FBP	FWCM	FBP	FWCM	FBP
0	-1.0000000000	0	0	0	0	0	0
0.05	-0.9987502604	9.46×10^{-7}	-	1.45×10^{-9}	-	4.44×10^{-13}	-
0.10	-0.9950041653	1.69×10^{-6}	7.50×10^{-5}	2.37×10^{-9}	1.30×10^{-7}	8.94×10^{-13}	1.22×10^{-11}
0.15	-0.9887710779	2.45×10^{-6}	-	3.18×10^{-9}	-	1.31×10^{-13}	-
0.20	-0.9800665778	3.25×10^{-6}	3.02×10^{-5}	3.89×10^{-9}	7.26×10^{-8}	1.69×10^{-13}	9.91×10^{-12}
0.25	-0.9689124217	4.06×10^{-6}	-	4.52×10^{-9}	-	2.08×10^{-13}	-
0.30	-0.9553364891	4.77×10^{-6}	2.71×10^{-5}	5.14×10^{-9}	4.04×10^{-8}	2.49×10^{-13}	7.20×10^{-12}
0.35	-0.9393727128	5.30×10^{-6}	-	5.83×10^{-9}	-	2.90×10^{-13}	-
0.40	-0.9210609942	5.67×10^{-6}	5.41×10^{-5}	6.52×10^{-9}	1.04×10^{-7}	3.31×10^{-13}	6.56×10^{-12}
0.45	-0.9004471024	6.13×10^{-6}	-	7.14×10^{-9}	-	3.69×10^{-13}	-
0.50	-0.8775825619	7.23×10^{-6}	1.12×10^{-3}	8.11×10^{-9}	2.35×10^{-6}	4.21×10^{-13}	7.58×10^{-10}

Table 9. Numerical comparison for $\mathscr{X}_2(\xi)$ with FWCM with Exact solution Problem 4.

ξ	Exact solution	$\|e_{1,4}(\xi)\|$		$\|e_{1,6}(\xi)\|$		$\|e_{1,9}(\xi)\|$	
		FWCM	FBP	FWCM	FBP	FWCM	FBP
0	1.0000000000	0	0	0	0	0	0
0.05	0.0499375130	7.85×10^{-6}	-	7.87×10^{-9}	-	4.07×10^{-12}	-
0.10	0.0995004165	6.92×10^{-6}	3.12×10^{-5}	5.64×10^{-9}	6.88×10^{-8}	3.30×10^{-12}	3.55×10^{-12}
0.15	0.1483156617	4.71×10^{-6}	-	5.50×10^{-9}	-	3.53×10^{-12}	-
0.20	0.1960133156	4.15×10^{-6}	4.91×10^{-5}	6.08×10^{-9}	1.19×10^{-7}	3.43×10^{-12}	1.04×10^{-11}
0.25	0.2422281054	5.16×10^{-6}	-	5.77×10^{-9}	-	3.44×10^{-12}	-
0.30	0.2866009467	6.15×10^{-6}	8.39×10^{-5}	5.45×10^{-9}	1.60×10^{-7}	3.44×10^{-12}	1.59×10^{-11}
0.35	0.3287804495	5.58×10^{-6}	-	6.00×10^{-9}	-	3.32×10^{-12}	-
0.40	0.3684243976	3.37×10^{-6}	1.16×10^{-4}	5.82×10^{-9}	2.16×10^{-7}	3.52×10^{-12}	2.06×10^{-11}
0.45	0.4052011961	2.39×10^{-6}	-	3.55×10^{-9}	-	2.73×10^{-12}	-
0.50	0.4387912809	9.88×10^{-6}	2.00×10^{-4}	1.11×10^{-8}	7.61×10^{-7}	6.68×10^{-12}	1.47×10^{-11}

Table 10. Numerical comparison for $\mathscr{X}_3(\xi)$ with FWCM with Exact solution Problem 4.

ξ	Exact solution	$\|e_{1,4}(\xi)\|$		$\|e_{1,6}(\xi)\|$		$\|e_{1,9}(\xi)\|$	
		FWCM	FBP	FWCM	FBP	FWCM	FBP
0	0.0000000000	0	0	0	0	0	0
0.05	0.0499791692	2.16×10^{-6}	-	1.65×10^{-9}	-	7.33×10^{-13}	-
0.10	0.0998334166	2.27×10^{-6}	3.70×10^{-5}	1.52×10^{-9}	9.54×10^{-8}	7.66×10^{-13}	1.43×10^{-10}
0.15	0.1494381325	1.96×10^{-6}	-	1.63×10^{-9}	-	9.23×10^{-13}	-
0.20	0.1986693308	1.92×10^{-6}	4.18×10^{-5}	1.84×10^{-9}	1.05×10^{-7}	1.01×10^{-12}	1.81×10^{-10}
0.25	0.2474039593	2.18×10^{-6}	-	1.89×10^{-9}	-	1.09×10^{-12}	-
0.30	0.2955202067	2.46×10^{-6}	3.54×10^{-5}	1.88×10^{-9}	9.70×10^{-8}	1.15×10^{-12}	1.68×10^{-10}
0.35	0.3428978075	2.41×10^{-6}	-	1.97×10^{-9}	-	1.17×10^{-12}	-
0.40	0.3894183423	1.98×10^{-6}	3.88×10^{-5}	1.95×10^{-9}	8.13×10^{-8}	1.21×10^{-12}	9.89×10^{-11}
0.45	0.4349655341	1.66×10^{-6}	-	1.59×10^{-9}	-	1.13×10^{-12}	-
0.50	0.4794255386	2.80×10^{-6}	2.08×10^{-4}	2.33×10^{-9}	7.03×10^{-7}	1.44×10^{-12}	1.37×10^{-9}

Table 11. Numerical comparison for $\mathscr{X}_1(\xi)$ with FWCM with Exact solution Problem 4.

ξ	AE of FWCM					
	k=1,M=4	k=2,M=4	k=1,M=6	k=1,M=6	k=1,M=8	k=2,M=8
0	0	0	0	0	0	0
0.05	3.16×10^{-5}	9.46×10^{-7}	1.10×10^{-7}	1.45×10^{-9}	2.30×10^{-10}	4.44×10^{-13}
0.10	5.78×10^{-5}	1.69×10^{-6}	2.00×10^{-7}	2.37×10^{-9}	4.27×10^{-10}	8.94×10^{-13}
0.15	8.10×10^{-5}	2.45×10^{-6}	2.89×10^{-7}	3.18×10^{-9}	6.38×10^{-10}	1.31×10^{-13}
0.20	1.03×10^{-4}	3.25×10^{-6}	3.84×10^{-7}	3.89×10^{-9}	8.56×10^{-10}	1.69×10^{-12}
0.25	1.25×10^{-4}	4.06×10^{-6}	4.81×10^{-7}	4.52×10^{-9}	1.06×10^{-9}	2.08×10^{-12}
0.30	1.48×10^{-4}	4.77×10^{-6}	5.78×10^{-7}	5.14×10^{-9}	1.26×10^{-9}	2.49×10^{-12}
0.35	1.71×10^{-4}	5.30×10^{-6}	6.68×10^{-7}	5.83×10^{-9}	1.44×10^{-9}	2.90×10^{-12}
0.40	1.91×10^{-4}	5.67×10^{-6}	7.52×10^{-7}	6.52×10^{-9}	1.62×10^{-9}	3.31×10^{-12}
0.45	2.19×10^{-4}	6.13×10^{-6}	8.28×10^{-7}	7.14×10^{-9}	1.80×10^{-9}	3.69×10^{-12}
0.50	2.42×10^{-4}	7.23×10^{-6}	8.99×10^{-7}	8.11×10^{-9}	1.98×10^{-9}	4.21×10^{-12}

Table 12. Numerical comparison for $\mathscr{X}_2(\xi)$ with FWCM with Exact solution Problem 4.

ξ	AE of FWCM					
	k=1,M=4	k=2,M=4	k=1,M=6	k=1,M=6	k=1,M=8	k=2,M=8
0	0	0	0	0	0	0
0.05	1.66×10^{-4}	7.85×10^{-6}	8.30×10^{-7}	7.87×10^{-9}	2.03×10^{-9}	4.07×10^{-12}
0.10	2.27×10^{-4}	6.92×10^{-6}	9.11×10^{-7}	5.64×10^{-9}	1.88×10^{-9}	3.30×10^{-12}
0.15	2.28×10^{-4}	4.71×10^{-6}	7.72×10^{-7}	5.50×10^{-9}	1.58×10^{-9}	3.53×10^{-12}
0.20	1.99×10^{-4}	4.15×10^{-6}	6.48×10^{-7}	6.08×10^{-9}	1.52×10^{-9}	3.43×10^{-12}
0.25	1.63×10^{-4}	5.16×10^{-6}	6.05×10^{-7}	5.77×10^{-9}	1.57×10^{-9}	3.44×10^{-12}
0.30	1.33×10^{-4}	6.15×10^{-6}	6.22×10^{-7}	5.45×10^{-9}	1.60×10^{-9}	3.44×10^{-12}
0.35	1.15×10^{-4}	5.58×10^{-6}	6.57×10^{-7}	6.00×10^{-9}	1.58×10^{-9}	3.32×10^{-12}
0.40	1.12×10^{-4}	3.37×10^{-6}	6.74×10^{-7}	5.82×10^{-9}	1.53×10^{-9}	3.52×10^{-12}
0.45	1.20×10^{-4}	2.39×10^{-6}	6.58×10^{-7}	3.55×10^{-9}	1.50×10^{-9}	2.73×10^{-12}
0.50	1.34×10^{-4}	9.88×10^{-6}	6.20×10^{-7}	1.11×10^{-8}	1.49×10^{-8}	6.68×10^{-12}

Table 13. Numerical comparison for $\mathscr{Z}_3(\xi)$ with FWCM with Exact solution Problem 4.

ξ	AE of FWCM					
	k=1,M=4	k=2,M=4	k=1,M=6	k=1,M=6	k=1,M=8	k=2,M=8
0	0	0	0	0	0	0
0.05	5.28×10^{-5}	2.16×10^{-6}	1.97×10^{-7}	1.65×10^{-9}	3.96×10^{-10}	7.33×10^{-13}
0.10	7.85×10^{-5}	2.27×10^{-6}	2.52×10^{-7}	1.52×10^{-9}	4.57×10^{-10}	7.76×10^{-13}
0.15	8.70×10^{-5}	1.96×10^{-6}	2.55×10^{-7}	1.63×10^{-9}	4.71×10^{-10}	9.23×10^{-13}
0.20	8.58×10^{-5}	1.92×10^{-6}	2.51×10^{-7}	1.84×10^{-9}	5.02×10^{-10}	1.01×10^{-12}
0.25	8.02×10^{-5}	2.18×10^{-6}	2.53×10^{-7}	1.89×10^{-9}	5.41×10^{-10}	1.09×10^{-12}
0.30	7.32×10^{-5}	2.46×10^{-6}	2.61×10^{-7}	1.88×10^{-9}	5.68×10^{-10}	1.15×10^{-12}
0.35	6.84×10^{-5}	2.41×10^{-6}	2.69×10^{-7}	1.97×10^{-9}	5.79×10^{-10}	1.17×10^{-12}
0.40	6.48×10^{-5}	1.98×10^{-6}	2.72×10^{-7}	1.95×10^{-9}	5.77×10^{-10}	1.21×10^{-12}
0.45	6.28×10^{-5}	1.66×10^{-6}	2.65×10^{-7}	1.59×10^{-9}	5.66×10^{-10}	1.13×10^{-12}
0.50	6.15×10^{-5}	2.80×10^{-6}	2.50×10^{-7}	2.33×10^{-9}	5.48×10^{-10}	1.44×10^{-12}

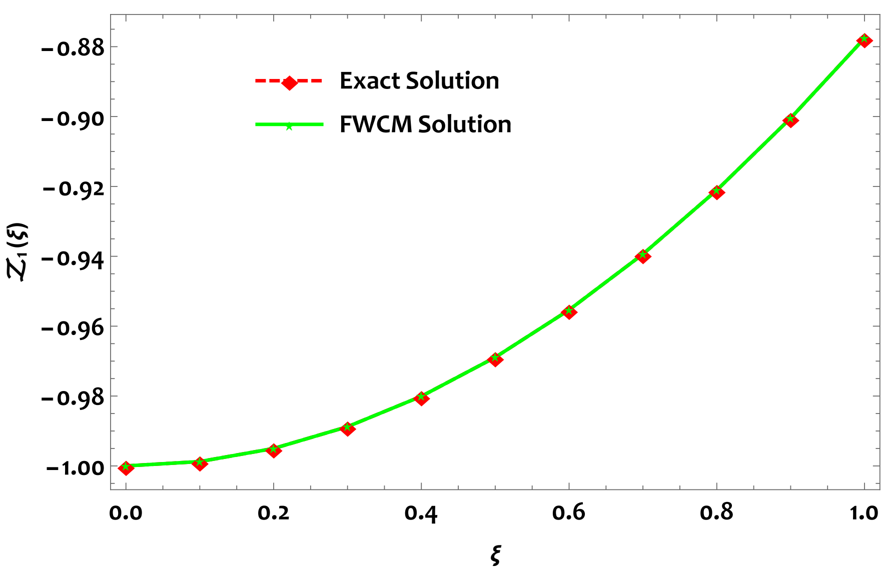

Figure 11. Graphical comparision of the FWCM solution $\mathscr{Z}_1(\xi)$ for Problem 4.

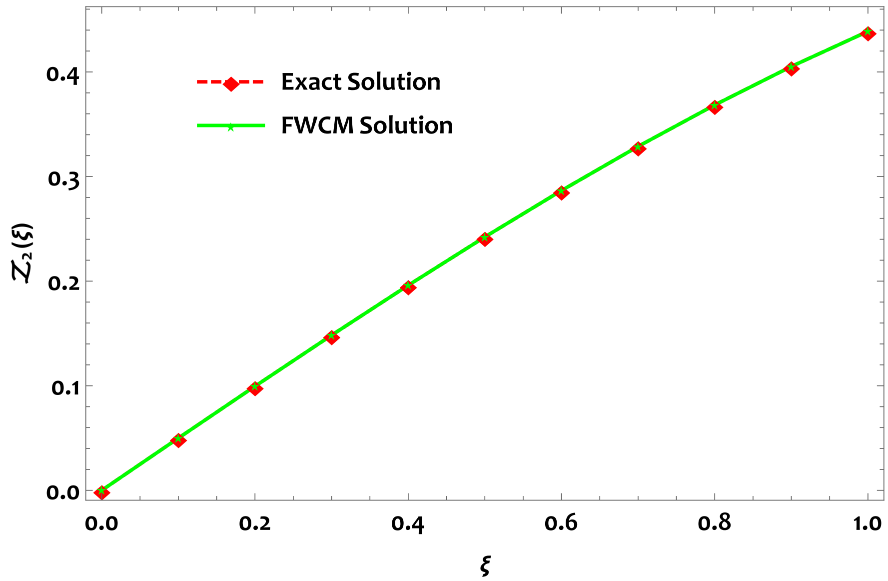

Figure 12. Graphical comparision of the FWCM solution $\mathscr{Z}_2(\xi)$ for Problem 4.

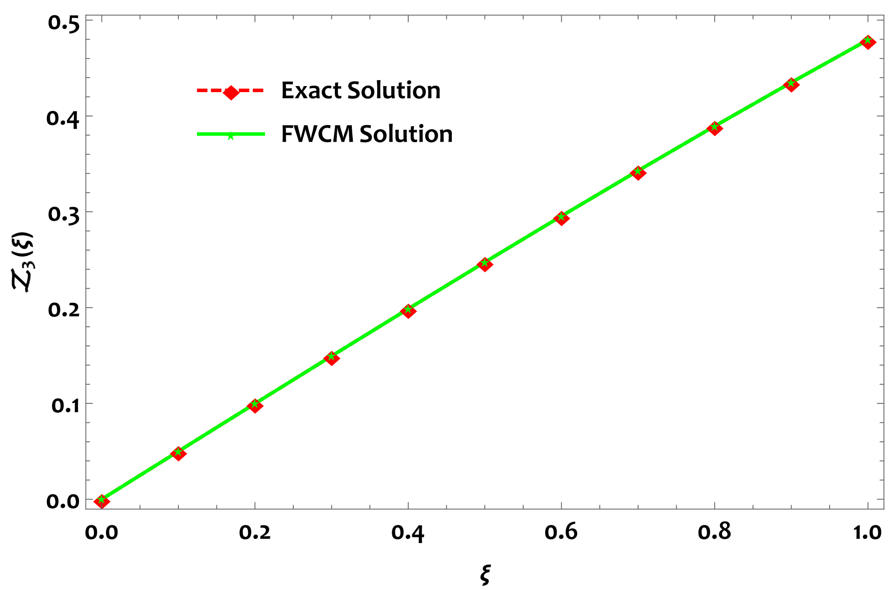

Figure 13. Graphical comparision of the FWCM solution $\mathscr{Z}_3(\xi)$ for Problem 4.

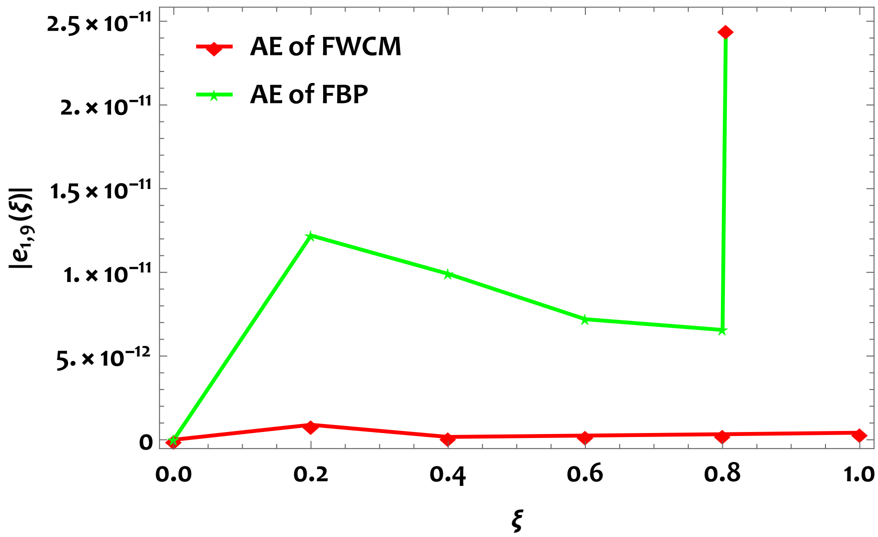

Figure 14. Plot of Absoute error (A.E) of the solution $\mathscr{X}_1(\xi)$ for Problem 4.

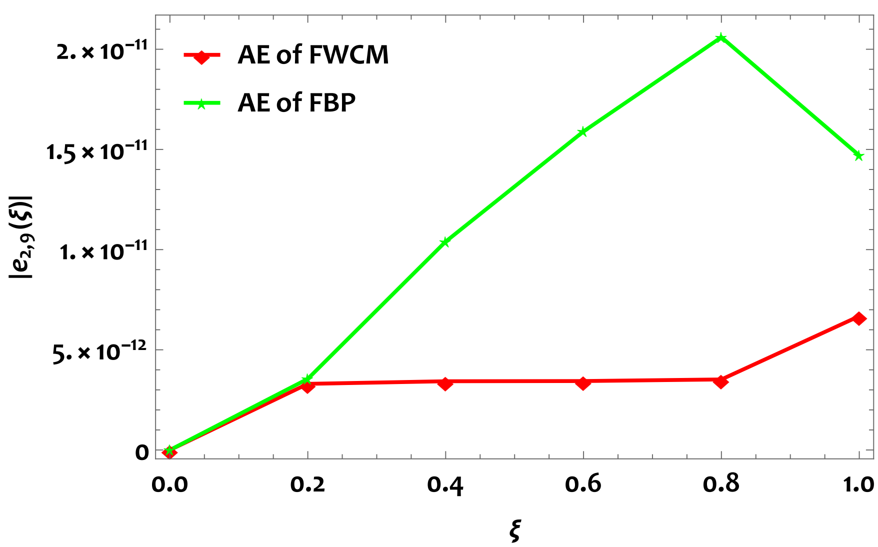

Figure 15. Plot of Absoute error (A.E) of the solution $\mathscr{X}_2(\xi)$ for Problem 4.

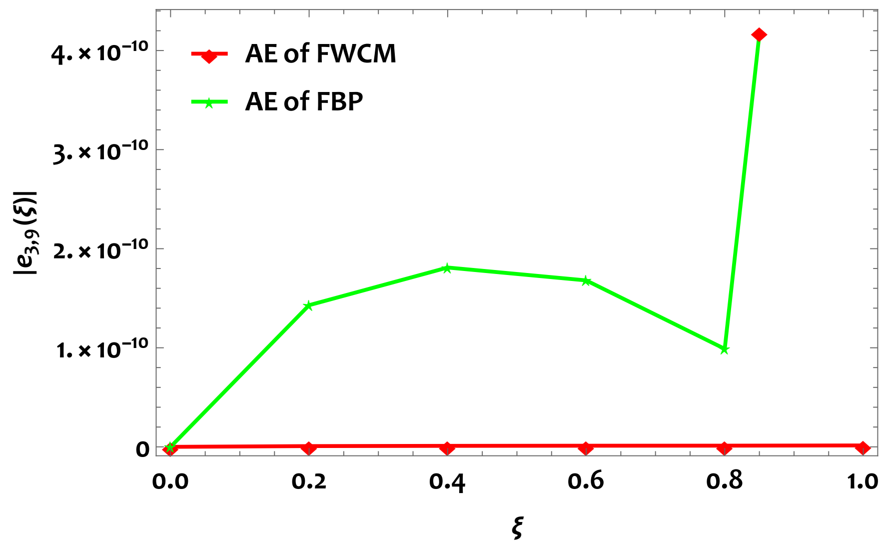

Figure 16. Plot of Absoute error (A.E) of the solution $\mathscr{Z}_3(\xi)$ for Problem 4.

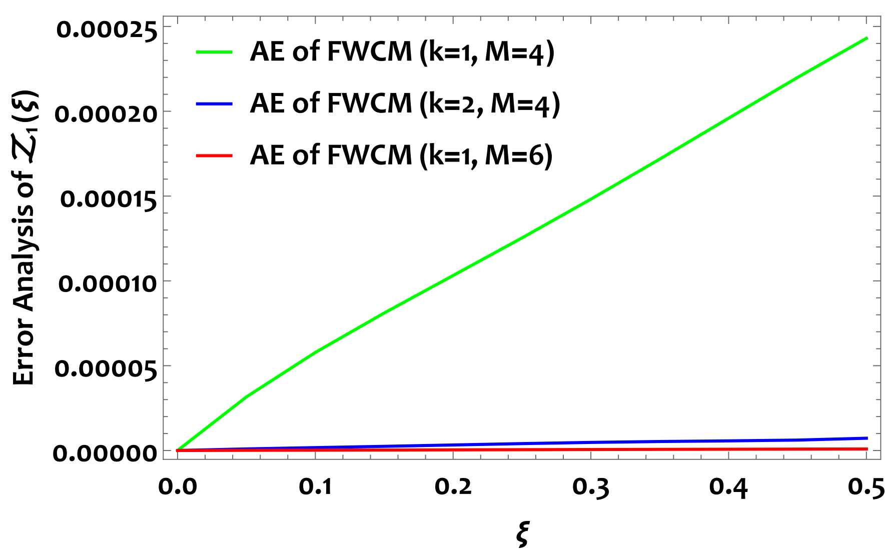

Figure 17. Comparision of Absoute error (A.E) of the solution $\mathscr{Z}_1(\xi)$ at different values and M and k for Problem 4.

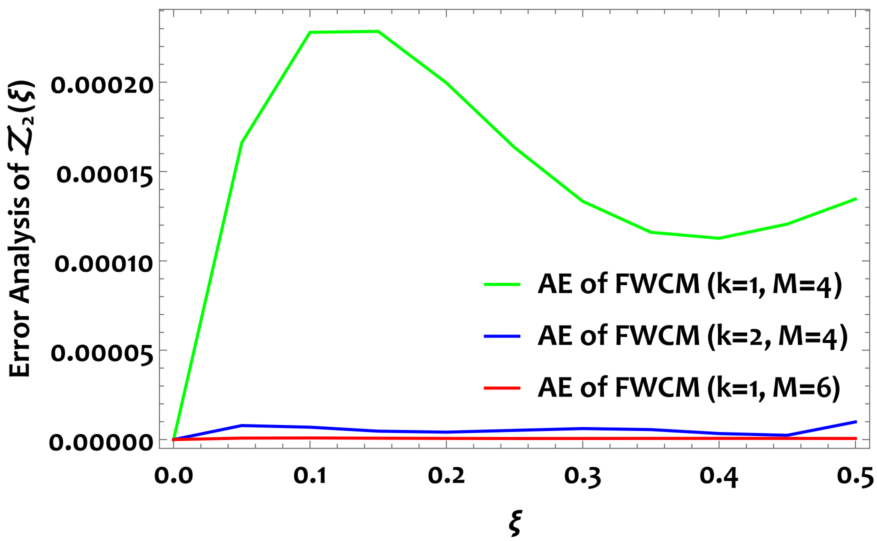

Figure 18. Comparision of Absoute error (A.E) of the solution $\mathscr{Z}_2(\xi)$ at different values and M and k for Problem 4.

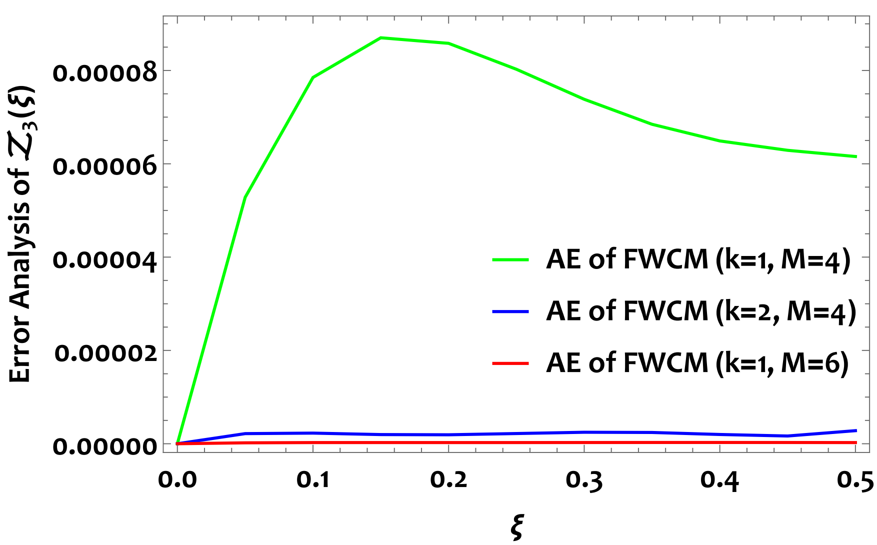

Figure 19. Comparision of Absoute error (A.E) of the solution $\mathscr{Z}_3(\xi)$ at different values and M and k for Problem 4.

7. Conclusion

In the present study, we developed the operational integration matrix for the Fibonacci wavelet and generated a novel technique called FWCM. This operational matrix served as our tool for estimating the numerical solution of the Pantograph-type differential equations under various physical conditions. Our numerical results are compared with the Fibonacci collocation method (FCM), First Boubaker Polynomials (FBP), Adomian decomposition method (ADM), and the exact solution through tables and graphs. Here, we attempted the four nonlinear problems of first and second order with different physical conditions. FWCM works well for all the four problems. Numerical approximations of the solutions and absolute errors of the method are tabulated in Tables 1-5 and 8-10. Graphical representations of the solutions are visualized in Figures 1-4, 7-8, and 11-13. Also, FWCM solutions are calculated at diverse values of M. By increasing the values of M, we get more accuracy in the solution, which can be seen in Tables 6-7 and 11-13. It shows that increasing M can obtain a higher-order accuracy. The tables and figures show that the suggested approach provides superior accuracy over the current numerical methods. Our computed result shows that, compared to other methods, our proposed approach is valuable and precise.

Declarations

Availability of Data and Materials: The data supporting this study's findings are available within the article.
Competing interests: The authors declare that they have no competing interests.
Author's contributions: KS proposed the main idea of this paper. KS and MG prepared the manuscript and performed all the steps of the proofs in this research. Both authors contributed equally and significantly to writing this paper. Both authors read and approved the final manuscript.
Conflict of interest: The author declares no conflict of interest.
Funding: The author states that no funding is involved.

Acknowledgements

The author expresses his affectionate thanks to the DST-SERB, Govt. of India. New Delhi for the financial support under Empowerment and Equity Opportunities for Excellence in Science for 2023-2026. F.No.EEQ/2022/620 Dated:07/02/2023.

References

[1] W. Sabir, and M. A. Koroma, *Approximation algorithm for a system of pantograph equations*, Journal of Applied Mathematics, 2012, 1, 714681.

[2] K. Suheil, *A Laplace decomposition algorithm applied to a class of nonlinear differential equations*, Journal of applied mathematics, 2002, 141–155.

[3] C. Musa, and S. Alkan. *A numerical method for solving a class of systems of nonlinear Pantograph differential equations*, Alexandria Engineering Journal, 2022, 61(4), 2651–2661.

[4] H. J. Huan, and H. Latifizadeh, *A general numerical algorithm for nonlinear differential equations by the variational iteration method*, International Journal of Numerical Methods for Heat and Fluid Flow, 2020, 30(11), 4797–4810.

[5] R. Dimple, and V. Mishra, *Numerical inverse Laplace transform based on Bernoulli polynomials operational matrix for solving nonlinear differential equations*, Results in Physics, 2020, 16, 102836.

[6] O. Zaid, *An optimized decomposition method for nonlinear ordinary and partial differential equations*, Physica A: Statistical Mechanics and its Applications, 2020, 541, 123323.

[7] O. Zaid, *An improved optimal homotopy analysis algorithm for nonlinear differential equations*, Journal of Mathematical Analysis and Applications, 2020, 488(2), 124089.

[8] D. Sara, and J. Rashidinia, *Solution of a system of delay differential equations of multi pantograph type*, Journal of Taibah University for Science, 2017, 11(6), 1141–1157.

[9] R. Parisa, Y. Ordokhani, and E. Babolian. *Muntz-Legendre wavelet operational matrix of fractional-order integration and its applications for solving the fractional pantograph differential equations*, Numerical Algorithms, 2018, 77, 1283–1305.

[10] M. Fakhrodin, and M. M. Hosseini, *A new Legendre wavelet operational matrix of derivative and its applications in solving the singular ordinary differential equations*, Journal of the Franklin Institute, 2011, 348(8), 1787–1796.

[11] E. Keshavarz, Y. Ordokhani, and M. Razzaghi, *The Taylor wavelets method for solving the initial and boundary value problems of Bratu-type equations*, Applied Numerical Mathematics, 2018, 128, 205–216.

[12] G. Manohara, S. Kumbinarasaiah, *Numerical solution of some stiff systems arising in chemistry via Taylor wavelet collocation method*, Journal of Mathematical Chemistry, 2023, 1–38.

[13] S. C. Shiralashetti, S. Kumbinarasaiah, *Hermite wavelets operational matrix of integration for the numerical solution of nonlinear singular initial value problems*, Alexandria engineering journal, 2018, 57(4), 2591–2600.

[14] K. Sunil, S. Ghosh, R. Kumar, and M. Jleli, *A fractional model for population dynamics of two interacting species by using spectral and Hermite wavelets methods*, Numerical Methods for Partial Differential Equations, 2021, 37(2), 1652–1672.

[15] C. Ibrahim, *Chebyshev Wavelet collocation method for solving generalized Burgers-Huxley equation*, Mathematical methods in the applied sciences, 2016, 39(3), 366–377.

[16] Z. Fengying, and X. Xu, *The third kind Chebyshev wavelets collocation method for solving the time-fractional convection diffusion equations with variable coefficients*, Applied Mathematics and Computation, 2016, 280, 11–29.

[17] S. C. Shiralashetti, S. Kumbinarasaiah, *Laguerre wavelets collocation method for the numerical solution of the Benjamina-Bona-Mohany equations*, Journal of Taibah University for science, 2018, 13(1), 9–15.

[18] Z. Fengying, and X. Xu, *Numerical solutions for the linear and nonlinear singular boundary value problems using Laguerre wavelets*, Advances in Difference Equations, 2016, 1, 1–15.

[19] P. Rahimkhani, Y. Ordokhani, E. Babolian, *Fractional-order Bernoulli wavelets and their applications*, Applied mathematical modelling, 2016, 40(17-18), 8087–8107.

[20] S. Kumbinarasaiah, G. Manohara, G. Hariharan, *Bernoulli wavelets functional matrix technique for a system of nonlinear singular Lane Emden equations*, Mathematics and Computers in Simulation, 2023, 204, 133–165.

[21] S. Kumbinarasaiah, S., R. Yeshwanth, *A study on Chlamydia transmission in United States through the Haar wavelet technique*, Results in Control and Optimization, 2016, 100396.

[22] S. Kumbinarasaiah, G. Manohara, *Modified Bernoulli wavelets functional matrix approach for the HIV infection of CD4+ T cells model*, Results in Control and Optimization, 2023, 10, 100197.

[23] Y. H. Youssri, W. M. Abd-Elhameed, E. H. Doha, *Ultraspherical wavelets method for solving Lane-Emden type equations*, Romanian Journal of Physics, 2015, 60(9-10), 1298–1314.

[24] M. Mallanagoud, and K. Srinivasa, *A novel approach for Benjamin-Bona-Mahony equation via ultraspherical wavelets collocation method*, International Journal of Mathematics and Computer in Engineering, 2024.

[25] S. C. Shiralashetti, S. Kumbinarasaiah, *Cardinal b-spline wavelet based numerical method for the solution of generalized Burgers-Huxley equation*, International journal of applied and computational mathematics, 2018, 4, 1–13.

[26] G. Manohara, and S. Kumbinarasaiah, *Numerical approximation of the typhoid disease model via Genocchi wavelet collocation method*, Journal of Umm Al-Qura University for Applied Sciences, 2024, 1–16.

[27] H. M. Srivastava, H. A. Shah, R. Abass, *An application of the Gegenbauer wavelet method for the numerical solution of the fractional Bagley-Torvik equation*, Russian Journal of Mathematical Physics, 2019, 26(1), 77–93.

[28] K. Thomas, *Fibonacci and Lucas numbers with applications*, Wiley. 2019, 1.

[29] F. A. Shah, M. Irfan, K. S. Nisar, R. T. Matoog, and E. E. Mahmoud, *Fibonacci wavelet method for solving time-fractional telegraph equations with Dirichlet boundary conditions*, Results in Physics, 2021, 24, 104123.

[30] G. Manohara, S. Kumbinarasaiah, *Numerical solution of a modified epidemiological model of computer viruses by using Fibonacci wavelets*, The Journal of Analysis, 2023, 1-26.

[31] S. Sabermahani, Y. Ordokhani, *Fibonacci wavelets and Galerkin method to investigate fractional optimal control problems with bibliometric analysis*, Journal of Vibration and Control, 2021, 27(15-16), 1778–1792.

[32] M. Irfan, and F. A. Shah, *Fibonacci wavelet method for solving the time-fractional bioheat transfer model*, Optik, 2021, 241, 167084.

[33] G. Manohara, S. Kumbinarasaiah, *Fibonacci wavelets operational matrix approach for solving chemistry problems*, Journal of Umm Al-Qura University for Applied Sciences, 2023, 1–18.

[34] S. Sabermahani, Y. Ordokhani, S. A. Yousefi, *Fibonacci wavelets and their applications for solving two classes of time-varying delay problems*, Optimal Control Applications and Methods, 2020, 41(2), 395–416.

[35] A. Sertan, and M. Cakmak, *Fibonacci collocation method for solving a class of systems of nonlinear differential equations*, New Trends in Mathematical Sciences, 2021, 9(4), 11–24.

[36] M. Irfan, F. A. Shah, K. S. Nisar, *Fibonacci wavelet method for solving Pennes bioheat transfer equation*, International Journal of Wavelets, Multiresolution and Information Processing, 2021, 19(6), 2150023.

[37] G. Manohara, S. Kumbinarasaiah, *Fibonacci wavelet collocation method for the numerical approximation of fractional order Brusselator chemical model*, Journal of Mathematical Chemistry, 2023, 1–31.

[38] K. Ayse, S. Yalcinbas, and M. Sezer, *Fibonacci Collocation Method for Solving High-Order Linear Fredholm Integro-Differential-Difference Equations*, International Journal of Mathematics and Mathematical Sciences, 2013, 1, 486013.

[39] S. Sabermahani, Y. Ordokhani, P. Rahimkhani, *Application of two-dimensional fibonacci wavelets in fractional partial differential equations arising in the financial market*, International Journal of Applied and Computational Mathematics, 2023, 8(3), 129.

[40] S. Sabermahani, Y. Ordokhani, *Solving distributed-order fractional optimal control problems via the Fibonacci wavelet method*, Journal of Vibration and Control, 2023, 30(1-2), 418–432.

[41] S. Randhir, and A. M. Wazwaz, *An efficient algorithm for solving coupled Lane-Emden boundary value problems in catalytic diffusion reactions The homotopy analysis method*, MATCH Communications in Mathematical and in Computer Chemistry, 2019, 81(3), 785–800.

[42] C. F. Chen, C. H. Hsiao, *Haar wavelet method for solving lumped and distributed-parameter systems*, IEE Proceedings-Control Theory and Applications, 1997, 144(1), 87–94.

[43] J. Majak, B. S. Shvartsman, M. Kirs, M. Pohlak, H. Herranen, *Convergence theorem for the Haar wavelet based discretization method*, Composite Structures, 2015, 126, 227–232.

[44] G. Manohara, and S. Kumbinarasaiah, *An innovative Fibonacci wavelet collocation method for the numerical approximation of Emden-Fowler equations*, Applied Numerical Mathematics, 2024, 201, 347–369.

[45] K. M. Altaf, S. Ullah, and S. Kumar, *A robust study on 2019-nCOV outbreaks through non-singular derivative*, The European Physical Journal Plus, 2021, 136, 1–20.

[46] S. Kumar, A. Kumar, B. Samet, and H. Dutta, *A study on fractional host-parasitoid population dynamical model to describe insect species*, Numerical Methods for Partial Differential Equations, 2021, 37, 2, 1673–1692.

[47] S. Kumar, R. P. Chauhan, S. Momani, S. Hadid, *Numerical investigations on COVID-19 model through singular and non-singular fractional operators*, Numerical Methods for Partial Differential Equations, 2024, 40(1), e22707.

[48] G. Behzad, and S. Kumar, *A study on fractional predator-prey-pathogen model with Mittag-Leffler kernel-based operators*, Numerical Methods for Partial Differential Equations, 2024, 40(1), e22689.

[49] K. Sunil, R. Kumar, S. Momani, and S. Hadid, *A study on fractional COVID-19 disease model by using Hermite wavelets*, Mathematical Methods in the Applied Sciences, 2023, 46(7), 7671–7687.

[50] S. Kumbinarasaiah, and R. A. Mundewadi. *Wavelets approach for the solution of nonlinear variable delay differential equations*, International Journal of Mathematics and Computer in Engineering, 2023.

[51] P. Veeresha, D. G. Prakasha, S. Kumar, *A fractional model for propagation of classical optical solitons by using nonsingular derivative*, Mathematical Methods in the Applied Sciences, 2020.